INVESTIGATION OF THE INTERACTIONS BETWEEN CANCER CELLS AND THE MICROENVIRONMENT AT THE CELLULAR LEVEL

A Thesis Submitted to
the Graduate School of Engineering and Science of
İzmir Institute of Technology
in Partial Fulfillment of the Requirement for the Degree of

MASTER OF SCIENCE

in Molecular Biology and Genetics

by
Eyüp YÖNDEM

June 2022
İZMİR

ACKNOWLEDGEMENT

I would like to thank my supervisor Prof. Dr. Devrim PESEN OKUR, for her limitless patience, understanding, encouragement, guidance, and support throughout this study. Additionally, I am glad to be a part of her laboratuvar members and take her experience to shed light on our ways.

I would like to thank my thesis defense committee members Assoc. Prof. Dr. Özden YALÇIN ÖZUYSAL, Asst. Prof. Dr. Dr. Yavuz OKTAY, Assoc.Prof. Dr. Gülistan MEŞE ÖZÇİVİCİ for their contributions.

I would like to express my deepest appreciation and thanks to the current members and alumni of the Controlled in vitro Microenvironments (CivM) Laboratory for their team spirit and support, especially Güncem O. UYSAL, and Helin GİRİŞ for their significant contributions to the completion of the study, and Dr.Gizem BATI, Dr. Abdurehman E. MOHAMMED, Dr. Aslı KISIM, D. Cemre TURGUT, Ceylan DEMİR, Dilan SAKİNCİ, Özge N. BELLİ, Mahmut ÇETİN, Ali A. DEMİR.

I also would like to thank Assoc. Prof. Dr. Gülistan MEŞE ÖZÇİVİ, Assoc. Prof. Dr. Özden YALÇIN ÖZUYSAL Laboratory members Yağmur C. ÜNAL, S. Şüheda YAŞARBAŞ, Z. Elif GÜNYÜZ, Eda EFE, Perge B. TOSUNOĞLU for their contributions and friendships.

I want to thank Zehra S. YILMAZ for her contributions.

Finally, I would like to express my greatest love, appreciation, and countless thanks to my family for their encouragement, understanding, help, and support during my whole life. Without their love, there would be no way for my success.

ABSTRACT

INVESTIGATION OF THE INTERACTIONS BETWEEN CANCER CELLS AND THE MICROENVIRONMENT AT THE CELLULAR LEVEL

Breast cancer is the most frequently diagnosed cancer type and the first leading cause of cancer-related deaths in women. Breast tumor mass is not only harboring cancer cells but also several types of stromal cells, including fibroblasts. While all of these stromal cells may have a calamitous effect on cancer progression, fibroblasts which make up nearly 80% of tumor mass present unique characteristics such as extensive extracellular matrix (ECM) production. In the context of tumors, the activated cells are referred to as cancer-associated fibroblasts (CAF), expressing several markers such as αSMA, FSP1, FAP, vimentin, and PDGFRβ. However, an in-depth understanding of the transdifferentiation of fibroblasts to CAFs is lacking.

ECM components may change when cells become cancerous, which can alter cell behavior, facilitating proliferation, differentiation, and migration. Decellularized ECM(dECM) has recently been considered one of the tools to study in-vitro cell-ECM interaction. In this work, we utilized cancer cell-derived ECM(ccECM) to investigate its effect on the differentiation of the fibroblast to CAFs by compering decellularization methods called the extraction buffer and the freeze-thaw cycle.

Our study suggested that ccECM from MDA-MB-231 impacted the fibroblasts' behavior from proliferation to differentiation via its ECM components, including fibronectin and laminin. The fibroblasts cultured on ccECM showed increased CAFs markers indicated above.

Overall, ccECM could be one of the intermediate steps in fibroblast differentiation, but in the future, the factors present in ccECM should be scrutinized to understand the mechanisms behind this effect.

ÖZET

KANSER HÜCRELERİ İLE MİKROÇEVRE ARASINDAKİ ETKİLEŞİMLERİN HÜCRESEL SEVİYEDE İNCELENMESİ

Meme kanseri en sık teşhis edilen kanser türü olmakla birlikte kadınlarda kansere bağlı ölümlerin birincil nedenidir. Meme tümörü kütlesi sadece kanser hücrelerini ihtiva etmekle kalmaz, aynı zamanda fibroblastlar dahil olmak üzere çeşitli stromal hücre türlerini de barındırır. Bu stromal hücrelerin tümü kanserin ilerlemesi üzerinde hayati bir etkiye sahip olsa da, tümör kütlesinin yaklaşık %80'ini oluşturan fibroblastlar, hücre dışı matris (ECM) üretimi gibi benzersiz özellikler sunar. Tümörler bağlamında, aktive edilmiş hücreler, aSMA, FSP1, FAP, vimentin ve PDGFRβ gibi çeşitli belirteçleri eksprese ederler ve kanserle ilişkili fibroblastlar (CAF) olarak adlandırılırlar. Bununla birlikte, fibroblastların CAF'lara nasıl dönüştüğü aydınlatılmayı beklemektedir.

ECM bileşenleri, hücreler kanserli hale geldiğinde değişebilir, bu da hücrelerin ona karşı cevabını değiştirip proliferasyonu, farklılaşmayı ve göçü kolaylaştırabilir. Hücresizleştirilmiş ECM(dECM) son zamanlarda in vitro hücre-ECM etkileşimini incelemek için araçlardan biri olarak kabul edilmiştir. Bu çalışmada, hücresizleştirme yöntemlerini, ekstraksiyon tamponunu ve donma-çözülmeyi karşılaştırarak fibroblastın CAF'lara farklılaşması üzerindeki etkisini araştırmak için kanser hücresinden türetilen ECM'i (ccECM) kullandık.

Çalışmamız, MDA-MB-231'den gelen ccECM'nin, fibronektin ve laminin dahil olmak üzere bileşenleri aracılığıyla fibroblastların proliferasyonundan farklılaşmaya kadar olan davranışlarını etkilediğini ileri sürdü. ccECM üzerinde kültürlenen fibroblastlar, yukarıda belirtilen artan CAF işaretleri gösterdi.

Genel olarak, ccECM, fibroblast farklılaşmasındaki ara basamaklardan biri olabilir, ancak gelecekte, ccECM'de bulunan faktörler, bu etkinin arkasındaki mekanizmaları anlamak için dikkatle incelenmelidir.

To my mother, my father, and myself,

To the dream and hope of homeless children…

TABLE OF CONTENTS

LIST OF FIGURES

Figure **Page**

LIST OF TABLES

CHAPTER 1.

INTRODUCTION

1.1. Cancer

Cancer is about to be the first leading cause of premature related death by superseding cardiovascular disease[1]. The latest estimation from the World Health Organization (WHO) in 2019 revealed that the prevalence of cancer varies between countries in which cancer is the first or second reason for cancer-related death in 112 of 183 countries before the age of 70. According to data estimated by GLOBOCAN, in 2020, 10 million deaths, including nonmelanoma skin cancer due to cancer, were recorded[2]. The distribution of cancer incidence and mortality may vary by continent and sexes. Indeed, the mortality rate in men is lung, prostate, and liver, whereas, in women, breast and cervical cancer are followed by lung[2]. Cancer is a progressive disease in which cells undergo continuous uncontrolled growth. When the cells transform into cancerous cells, they acquire some characteristics such as changes in genetic background[3], hijacking from apoptosis[4], losing contact inhibition[5], growing without external signal[6], and replicative immortalization, immune evasion, resistance to cell death, enabling to induce and access vasculature, capacity to invade and metastasize[6]. Human beings have been dealing with cancer and its treatments from the dawn of history because it is not a homogeneous but rather a heterogeneous disease that affects multiple organs and has different markers and pathology that vary from person to person. Even though treatments have been improving over the last decades with the help of technologies and the development of new systems to mimic better cancer's nature, such as the lab-on-a-chip platform and personalized medicine, we need to go beyond the limit in order to reveal new strategies upon cancer. Breast cancer is one cancer type that claims many lives, and many points are waiting to be brightened.

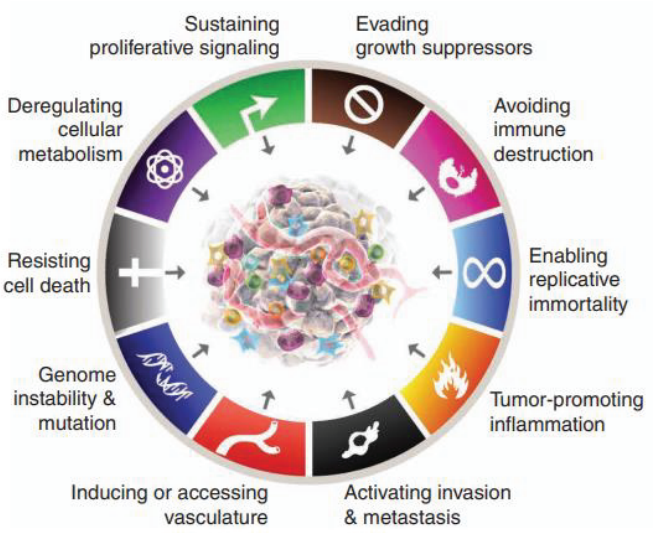

Figure 1. 1. Hallmarks of Cancer

(Source: Hanahan D[6])

1.2. Breast Cancer

As of 2020, breast cancer is the most frequently diagnosed cancer type among all cancer types, with 2,261,419 new cases. Indeed, it is now placed 5th leading cause of cancer-related death after lung, colorectal, liver, and stomach cancer in both sexes, but in women, it is in the first place with 684,996 deaths[2]. There has been an ascendant tendency in the global incidence of breast cancer, with 641,000 cases as of 1980[7]. Nearly five to 10% of breast cancers are associated with mutated genes coming from the parent, and the most common inherited germline mutations are BRCA1 and BRCA2, whose effect is cumulative[8-10]. Developing breast cancer is 72% and 69% when a woman has BRCA1, and BRCA2 mutated genes by the age of 80 years, respectively[11]. In addition to BRCA1 and BRCA2, a gene panel including TP53, PTEN, PALB2, STK11, and ATM was revealed by next-generation sequencing[9, 12]. Besides the inherited genes, several factors risk getting breast cancer, such as having first-degree relatives with breast cancer, race, and ethnicity, having dense breasts, early menstruation or late menopause and alcohol consumption, insufficient physical activity, and obesity[8, 13]. Thanks to these factors, we can understand how breast cancer arises, but the mechanism underlying breast tumors' occurrence is not yet apparent. At the beginning, two leading strategies are put on the stage about breast tumors.

The first is clonal evolution, in which any breast epithelial cell can undergo genetic and epigenetic alterations that cause tumor formation. The cancer stem cell model is the second one in which cancer and progenitor stem cells have the ability to initiate and maintain tumor progression[14, 15]. Although breast cancer can originate from any breast site, the majority of breast cancer arises in the functional unit of the breast, termed glandular tissue. [9]. The glandular tissue that is one of three basics unit of the breast with the adipose and connective tissue has 12 to 20 sections called lobes that harbor lobules at which the milk is produced and delivered to the nipple via ducts[9, 16]. Cancer arising in the epithelial cells is called a carcinoma, the most pronounced cancer of the breast's glandular tissue. The place where breast cancer types are named has two main categories: preinvasive, confined by the basement membrane, and invasive, which can invade the closer tissue through the breast stroma[17]. While the former subsumes ductal carcinoma in situ (DCIS) and lobular carcinoma in situ (LCIS), the latter involves the counterpart of DCIS and LCIS called ductal carcinoma and lobular carcinoma. Both ductal and lobular carcinoma originated in the lobes' lobular units, and they are by far the most organized and studied groups among the breast cancer types[18, 19]. The second categorization of breast cancer type is made by looking at their molecular profiles or intrinsic genes according to PAM50 results[20, 21]. These intrinsic subtypes are basal-like, Cloudin-low, HER2-enriched, luminal A, and luminal B. In contrast, basal-like and HER2-enriched subtypes have TP53, BRCA mutations, and HER2, GRB7, TOPO2, and MYC amplification; Luminal A and Luminal B have PIK3CA, ESR1, ERBB2, ERBB3 mutations, and ERS1, GATA3, FOXA1, XBP1 activation. The other subtype of intrinsic breast cancer is the Cloudin-low, mostly triple-negative and similar to basal-like subgroups[9, 22]. The third categorization of breast cancer is the surrogate intrinsic type related to their receptor expression and histological situation. These receptors are progesterone (PR), estrogen (ER), and human epidermal growth factor receptor-2 (HER-2) and proliferation marker (Ki67). Based on the expression pattern of these receptors, the first group is hormone-receptor-positive, which is subdivided into Luminal A (ER/PR+ and HER2-, low Ki67, good prognosis) and Luminal B-like HER2-/+ (ER/PR+, high Ki67, intermediate prognosis), and HER2-enriched (ER/PR-, HER2+, high Ki67, intermediate prognosis). Tumors with none of these markers fall into another group and are triple-negative breast cancer (TNBC) with a high Ki67 and poor prognosis[23].

Breast cancer, like other types of cancer, is not homogenously a collection of defective cells. It is heterogeneous and harbors different types of cells having different mutations and receptor situations. It is also under the effect of the tumor microenvironment (TME) and cells present in its stroma, making it complicated and mitigating the probability of getting a remedy by chemotherapy and radiotherapy. That is why the tumor and its microenvironment are under the scope.

1.3. The Tumor Microenvironment

Cancer is not a place where one can find only a single type of disordered cell; instead, it is an ecosystem with various cell types enabling cancer initiation to metastasis. The TME is a niche that comprises non-malignant host cells with the cellular and non-cellular compartment called the stroma[24]. As seed and soil theory indicated by Paget in 1889, a tumor needs a stroma that can be directed to progress and take advantage of the cell located in its surroundings. [25, 26]. In a healthy stroma, cells are under homeostasis by signaling pathways and secreted factors that provide communication between cells; hence there is harmony in cells and their environment[24]. There is an extracellular matrix(ECM), a chef as in an orchestra to connect cells and their microenvironment.

Moreover, ECM comprises a structure called basement membrane and interstitial ECM, whose role is to separate epithelial cells from others and communicate with stromal tissues by paracrine signaling, respectively[27]. Although the stroma has tumor suppressor ability, there are various cell types whose functions normally regulate and maintain the cellular compact. Still, those cells can evolve to contribute to tumor progression as cancer progresses in the tumor. For example, immune cells are customarily expected to be on our side when any pathogenic situation occurs, cancer as well. However, there is ample evidence that immune cells allow tumors to progress in every aspect as macrophages can turn into tumor-associated macrophages facilitating tumor rejection and enhancing angiogenesis, which is associated with poor prognosis[28-33]. Besides macrophages, several cell types are bystanders in the stroma that enhance angiogenesis, such as endothelial cells and pericytes, or are cytotoxic for cancer cells like effector natural killer cells.[34-36]

Although the TME involves cellular and non-cellular components, one more cell called fibroblast comprises 80% of stroma in breast cancer and nearly joins every step in tumor progression. The first description of fibroblast dates back to the 19th century, when

the location and appearance were seen under a microscope. It is defined as a cell synthesizing collagen residing in the connective tissue.[37, 38]. Additionally, fibroblasts can be derived either from mesenchyme yielding mesoderm or from the neural crest cells, and it presents spindle-shaped cells which are non-vascular, non-epithelial, and non-inflammatory[39, 40]. Because it originated from mesenchymal precursor cells, fibroblast has similarities with cells from the same lineage, such as adipocytes, chondroblasts, and osteoblasts. Thus, there is no unique marker when one wants to identify them. It seems that fibroblast-specific-protein-1 (FSP-1) is the most valid marker with cell shape and location in the stroma[41].

Studies in literature have put a new definition on the scene of fibroblasts which are resting mesenchymal cells capable of activating through proper signaling and characteristic similar to mesenchymal stem cells(MSCs)[40, 42]. Several tangible evidence identify the roles assigned to fibroblasts as properties for activated fibroblasts, myofibroblasts, and MSCs, such as contractility, proliferation, secretory and synthetic phenotype, and migration.[43]. Indeed, resting fibroblast is like a precursor for activated fibroblast, and they become active when they receive relevant growth factors like transforming growth factor-beta(TGFβ)[44]. Several proses activated the leading play in such as turnover of ECM, tissue repair, wound healing, fibrosis, and angiogenesis[45, 46]. One of the main functions of the activated fibroblast is holding connective tissue under homeostasis by secreting fibrillar ECM such as type I, III, V collagen and fibronectin, and basement membrane ECM components such as collagen type IV and laminin[47, 48]. In addition to secretion capacity, activated fibroblasts also have enzymes capable of degrading ECM proteins called matrix-Metallo proteases (MMPs), which yield a duty for activated fibroblasts to maintain the turnover of the extracellular matrix[49]. Furthermore, another role of activated fibroblasts in our body is to care for adjacent epithelial cells' homeostasis via secreting growth factors and cell-to-cell interaction with the mesenchymal-epithelial cell[50].

Moreover, apart from the physiological roles of activated fibroblast, they also impact pathological conditions like wound healing and tissue fibrosis. When the wound recovers, the number of activated fibroblasts decreases via apoptosis[45]. However, suppose we consider cancer as a wound that does not heal. In that case, it creates a reactive stroma with an increased number of activated fibroblasts recruited to the tumor site by cancer

and stromal cells, including fibroblasts via secretion growth factors such as TGFβ and PDGF[51-53]. The fibroblasts in tumor stroma are called a tumor or cancer-associated fibroblasts (TAFs or CAFs)[54].

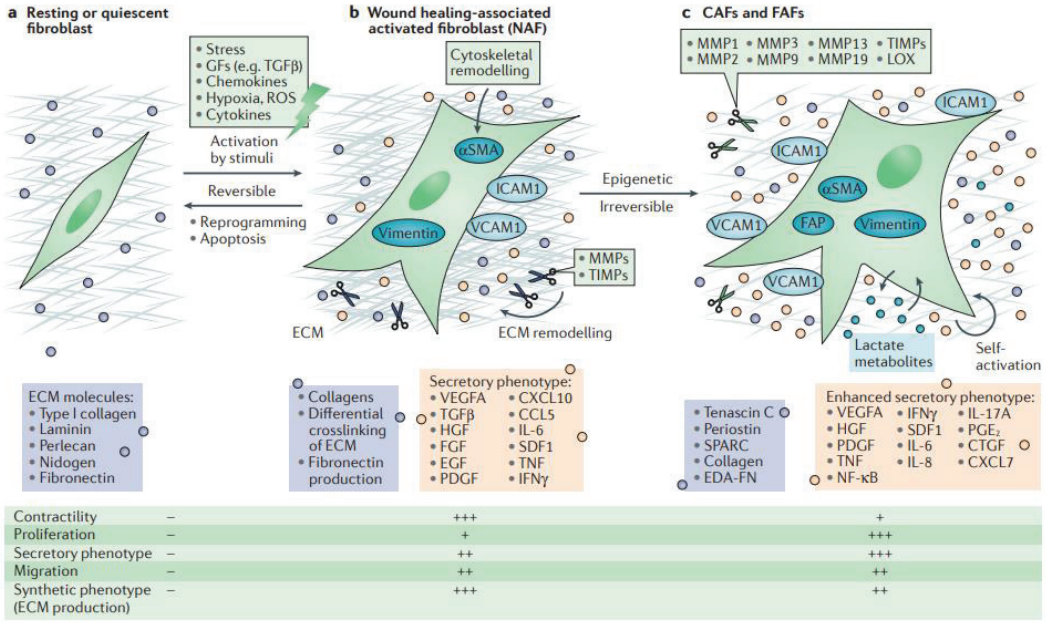

Figure 1. 2. Activation steps of fibroblasts

(Source: Kalluri R[40])

1.3.1. Cancer-Associated Fibroblast

The TME has a crucial role in tumor progression, and it harbors cancer cells and other stromal cell types, including activated fibroblasts called CAFs. When the fibroblasts turn into CAFs, they also provide a unique environment for the cancer cell to hijack immune cells and migrate through ECM utilizing the CAF secretory and synthetic phenotype. Even if studies have revealed that CAFs are the leading player in cancer progression when one considers defining them, it will be tricky due to the complexity of their origins and markers. It was initially described as myofibroblast in CAF subtypes thanks to alpha-smooth muscle actin (α-SMA) expression[55, 56]. Although they are similar to their counterparts, one can discriminate them from the toothed nuclei and multiple brunches of cytoplasm under light microscopy[57]. Further characterization of CAFs may

be validated by electron microscopy with their planer cell polarity, dense stress fiber, increased rough endoplasmic reticulum (ER), and free ribosomes[55].

The unique characteristic of CAFs is to create highly reactive stroma enabling ECM turnover with boosted production and degrading ECM proteins by MMPs. This ability of CAF accumulates various types of ECM proteins such as collagens, fibronectin, laminin, and tenascin-C, which may increase the stiffness of stroma. Indeed, increased stiffness can be a barrier to immune cells filtration and scaffold, helping the interaction of cancer cells with the stroma. The remodeling of ECM by CAF promotes cancer cell migration via its contractility and proteolysis capacity[58-60]. On the other hand, the degradation of ECM proteins by MMPs can allow vascular endothelial growth factor A (VEGFA) to interact with vascular endothelial growth factor receptors (VEGFRs), promoting angiogenesis[61]. On top of it, CAF secretes many growth factors, pro-inflammatory cytokines, and chemokines, promoting the proliferation of cancer cells and recruitment of immune-suppressive cells[62-64]. For example, CAFs secreting immune-modulatory factors such as C-X-C motif ligand CXCL(1,2,5,12), C-C motif ligand CC(5), IL(1β,6,12) are associated with TME regulation and recruitment of immune cells[65]. Moreover, it may promote cancer cell proliferation and metastatic spread by secreting fibroblast-growth factor-2 (FGF-2) and SDF1/CXCL12. CAFs can significantly affect tumor progression from initiation to colonizing cancer cells to the metastatic niche[66]. Yet, it has been debated where CAFs come from and what are the markers to define them.

1.3.2. CAF Heterogeneity and Plasticity

As in cancer cells, CAF populations in tumor stroma are not homogeneous but rather substantially heterogeneous[67]. Studies showed that this heterogeneity resulted from different sources for CAFs. The emergence of evidence has revealed that resident fibroblast can turn into CAF with the process governed by TGFβ and stromal-derived factor-1 (SDF-1) released from cancer cells[67]. Indeed, when TGFβ was administered to the rats, the fibroblast expressing α-SMA was increased[68, 69]. Studies have also dictated that CAF can evolve from resident fibroblast as in-vivo and in-vitro by inducing with TGFβ[70-80]. Another source of CAF is epithelial cells governed by epithelial to mesenchymal transition (EMT). Although the cancer cell's transition to CAF is debatable, a study published in 2002 indicated that cancer cells might acquire myofibroblast

characteristics governed by vimentin expression under appropriate conditions.[81]. Further studies also revealed that TGFβ might be the potential transducer for EMT to gain myofibroblast-like features for epithelial cells expressing fibroblast-specific protein-1 (FSP-1) and α-SMA[82-86]. Endothelial cells can evolve to myofibroblast by endothelial to mesenchymal transition (EndMT), at which the TGF-β also directs. Those endothelial cells present myofibroblast markers as in myofibroblast coming from epithelial cells[87-89]. There are also less common sources from which CAF can be originated; for example, under MDA-MB-231 and MCF-7 cancer cell line conditioned medium (CM), adipocytes-derived stem cells can gain increased α-SMA and Tenascin-C[90]. Finally, bone marrow-derived fibrocytes, mesenchymal stem cells, and smooth muscle cells can turn into CAF-like phenotypes through recruitment or transdifferentiation[91].

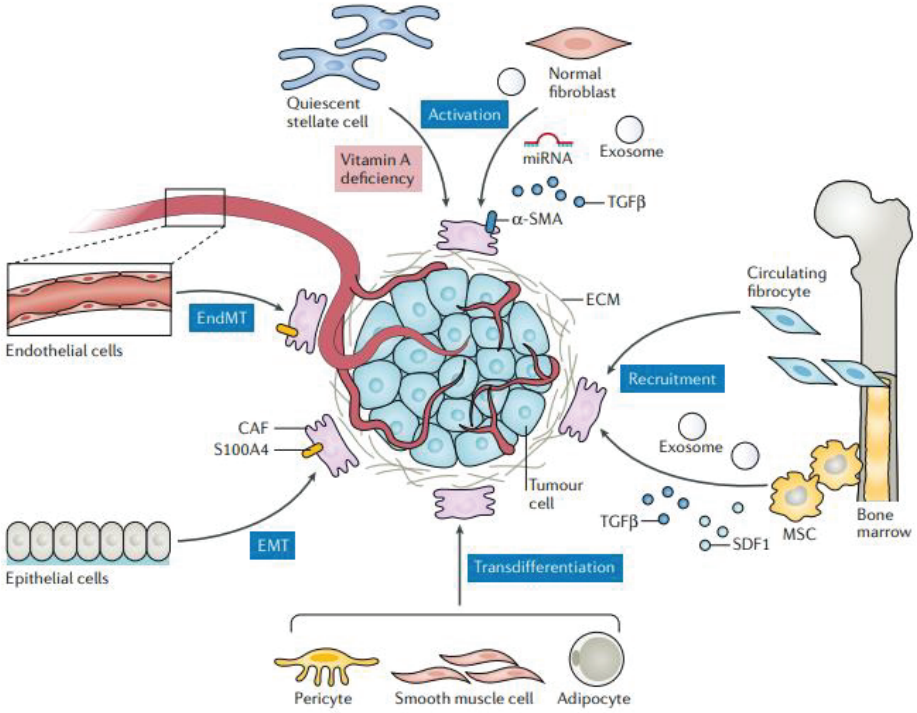

Figure 1. 3. Potential sources of Cancer-Associated Fibroblast

(Source: Chen X. and Song E[91].)

Another debating issue is the detection of CAFs because there is no such marker that is only associated with CAFs, rather several characteristics. Initially, myofibroblast having increased α-SMA is termed CAF. In addition to α-SMA, studies have revealed several CAF markers in the last two decades. The most common CAFs markers related to the cytoskeleton and cytoplasmic proteins are S100A4/FSP-1, vimentin, and desmin[91].

Some CAF markers can also rise in receptor and membrane-bound proteins such as FAP, PDGFRβ, Cavalin-1 (CAV1), CD10, Podoplanin (PDPN), or ECM components like tenascin-C, fibronectin, and laminin.[73, 91] Metanalysis and RNAseq data have recently demonstrated several CAF subtypes classified according to their expression markers. Studies have uncovered four subclasses named CAF-S1 to CAF-S4 of CAFs in breast, ovarian, and later lung cancer[65, 92, 93]. Indeed each subtype has a range of expression profiles with different functions. For example, CAF-S1 is more related to ECM remodeling and presents a FAP^{high}, $FSP\text{-}1^{medium}$, $PDGFR\beta^{medium}$, $\alpha\text{-}SMA^{medium}$, $CD29^{medium}$, and $CAV1^{low}$ expression. CAF-S4, on the other hand, is associated with perivascular regulation and shows a $CD29^{high}$, $\alpha\text{-}SMA^{high}$, $FSP\text{-}1^{low\text{-}medium}$, $PDGFR\beta^{low\text{-}medium}$, $CAV1^{low}$, and $FAP^{negative\text{-}low}$ expression. Conversely, CAF-S2 presents in luminal breast cancer, exhibiting a $FAP^{negative}$, $\alpha\text{-}SMA^{negative}$, $PDGFR\beta^{negative}$, $CAV1^{negative}$, $CD29^{low}$, and $FSP\text{-}1^{low\text{-}negative}$ expression. Compared with other subtypes, CAF-S3 is physiologically present in healthy tissue with a $FAP^{negative}$, $\alpha\text{-}SMA^{negative}$, $FSP\text{-}1^{medium\text{-}high}$, $PDGFR\beta^{medium}$, $CD29^{medium}$, and $CAV1^{low}$[94-96]. The FAP^{high} population of those subtypes yields two new subgroups named inflammatory CAF (iCAF) located in distance sites from the neoplastic cells and myofibroblastic CAF (mCAF) found near adjacent cells according to their low or increased expression of α-SMA, respectively[92-94, 96-98]. Furthermore, a comprehensive study by Lambrechts et al. revealed the existence of fibroblast clusters in patient samples. They showed that lung cancer harbors five fibroblast clusters named clusters 1, 2, 4, 5, 6, and 7, and all have distinct properties and expression profiles. For example, Cluster 1 enriched in adjacent neoplastic cells expresses high col10A1, EMT, and ECM proteins with the TGFβ-related genes, while cluster 6 found in non-malignant tissue exhibit collagen type I, III, V, and VII. Additionally, cluster 2 has higher expression of α-SMA and other genes related to myogenesis and angiogenesis, reflecting fibroblasts' activation[99].

Overall, CAF is one of the leading players in TME with various functions related to tumor progression from initiation to metastasis. Although mounting evidence has shown the existence of CAF from different sources, including resident fibroblast, the differentiation of fibroblast to CAF is still under investigation, and an in-depth understanding of the transdifferentiation of fibroblasts to CAFs is lacking. Utilizing cancer-cell-derived ECM (ccECM), we proposed fibroblast cultured on ccECM

differentiates to CAF via surface-immobilized proteins and soluble growth factors present in ccECM.

1.4. Aim of the Study

CAF is now remarkably under investigation to reveal its clinical value for preventing invasion, metastasis, and immune hijacking in various cancer types, including breast and lung cancer. Several known cellular processes such as EMT, wound healing and secreted factors like TGFβ participate in CAF differentiation. Although recent studies have focused on CAFs' heterogeneity and subtypes, it is unclear how CAF differentiate and create such a population pool. ECM is a robust cancer progression partner, facilitating cellular communication and migration. Several cell types present in TME, including fibroblasts, are highly regulatable. When the cells become cancerous, ECM contents may change and create an active stroma, yielding a meshwork helping cancer progressions.

In the light of comprehensive studies, this work aimed to shed light on the effect of ccECM on the differentiation of fibroblasts to CAF, creating a ccECM from the MDA-MB-231 TNBC cell line using extraction buffer and the freeze-thaw methods.

CHAPTER 2.

MATERIALS AND METHODS

2.1. Cell Culture

In this work, we used invasive triple-negative breast cancer cell line MDA-MB-231, a non-tumorigenic human breast epithelial cell line MCF-10A, and lung-derived fibroblast cell line WI38. All were acquired from ATCC. MDA-MB-231 cells, MCF-10A cells, and WI38 cells were cultured in high glucose Dulbecco's Modified Eagle Medium (DMEM) (Biological Industries (BI) ref# 01-055-1A), DMEM/F12 (BI, ref# 01-0170-1A), and MEM-ALPHA (BI, ref# 01-042-1A), respectively. DMEM and MEM-ALPHA mediums were supplemented with 10% Fetal Bovine Serum (FBS) (BI, Ref# 04-127-1A), 1% L-Glutamine (BI, ref# 03-020-1B), and 1% Penicillin/Streptomycin (P/S) (BI, ref# 03-031-1B) while MCF10A cells culture medium was supplemented with 5% Donor Horse Serum (DHS) (BI, ref# 04-004-1A), 20ng/ml EGF (Sigma, ref# E9644), 0.5ug/ml Hydrocortisone (Sigma, ref# H0888), 100ng/ml Cholore Toxin(Sigma, ref# C8052), 1% L-Glutamine, and 1% P/S. All cell lines were maintained at 37°C in a humidified incubator with 5% CO2.

MDA-MB-231 cells and WI38 cells were subcultured using 0.05% Trypsin-EDTA (BI, ref# 03-05-1B) in the humidified incubator at 37°C, 5% CO2 for 5 minutes, whereas MCF-10 cells were split using 0.25% Trypsin-EDTA (BI, ref# 03-050-1B) for 15 minutes in the same environment mentioned above.

2.2. Decellularized Cell-Derived ECM as a Scaffold

Decellularized ECM(dECM) has been utilized in order to develop tissue engineering thanks to its biocompatibility and bioactivity[100]. It was shown that dECM could alter cell behavior via its physicochemical signals capacity and biological performance[101]. Moreover, several studies utilized these events to produce a tissue-specific niche for subsequent experiments. For example, cell-derived ECM from embryonic stem cells provided them to differentiate and become more proliferative when

embryonic stem cells were seeded on their dECM[102]. It was also found that dECM from cells were able to differentiate other cell types, including endothelial and epithelial cells[103]. Although there were countless studies in the literature, it is not certain which procedure is appropriate for getting dECM which has been wholly purified from immunological components like cell nuclei. Several techniques have been used to obtain dECM having a mesh network, including the extraction buffer and the freeze-thaw method[101]. Hence, here we tried to utilize both methodologies in order to obtain well-organized and nuclei-free dECM.

2.3. Isolation of Cell-Derived Extracellular Matrix

2.3.1. Extraction Buffer

ECM deposition from individual experiments was kindly obtained according to optimization of published protocols[104]. Briefly, MDA-MB-231 cells were seeded at $5x10^4$ cells/cm^2onto the glass coverslips in 6-well plates and maintained for 3, 5, and 7 days within the humidified atmosphere at 5% CO2 and 37°C. The culture medium was replaced with half of the fresh medium every two days. Once culture time finished, the coverslips were kindly exposed to an extraction buffer including 20mM NH4OH(ref# 320145, sigma), 0.05% Triton X-100/ 1X Phosphate Buffer Saline (PBS) for 5 minutes, and they were observed under light microscopy until the cells were removed entirely.

2.3.2. The Freeze-Thaw

ECM deposition from individual experiments was kindly obtained according to optimization of published protocols[105]. Briefly, MDA-MB-231 cells were seeded at a ratio of $5x10^4$ cells/cm^2 onto the glass coverslips in 6-well plates and maintained for 3, 5, and 7 days within the humidified atmosphere at 5% CO2 and 37°C, and every two days, the culture medium was replaced with half of the fresh medium. Once cells on the coverslips were ready to experiment, the coverslips were gently transferred to new six-well plates to perform clear decellularization using the freeze-thaw. The coverslips transferred to six-well plates were washed with 1X PBS once and exposed to -80°C with 2ml of 1X PBS for 35 minutes, then they were exposed to warm 1X PBS until completely melted. After one freeze-thaw cycle, each well was rinsed with 1X PBS until cells were removed entirely, and a cell-free coverslip containing ccECM was used to culture

fibroblast cells following 200U/ml DNAse-1(# DN25, sigma) treatment for 60 minutes at 37°C.

2.4. Activation of Fibroblast

In our experimental setup for positive control, we use 10ng/ml TGFβ (ref# 781802, biolegend) to induce fibroblast to CAF differentiation. Wı38 cells were seeded onto coverslips using a serum-free medium and starved for 6 hours to increase the recruitment of TGFβ. After starvation, the serum-free medium was exchanged with Wı38 complete medium containing 10ng/ml TGFβ and cultured for 48 hours. Then, to see whether differentiation occurred or not, we applied an immunostaining assay and Q-RT-PCR using CAF markers indicating belove.

2.5. Immunostaining and Fluorescence Imaging

2.5.1. Staining for Fibroblast

Wı38 cells were cultured on decellularized coverslips containing ccECM and ccECM-free coverslips at 20,83x10^3cells/cm^2 for 48 hours to investigate whether ccECM activated fibroblasts. Cells were fixed using 4% paraformaldehyde (PFA) after the washing step with 1X PBS. Then, using 0.1% Triton X-100/PBS, cells were permeabilized for 5 minutes at room temperature (RT) after washing with 1X PBS three times each at 5 minutes intervals, and then cells were blocked with 5% goat serum (GS)/PBS for 60 minutes at RT. Permeabilized cells were exposed to the primary antibody/PBS using a CAF marker antibody sampler kit (#31549, cell signaling technologies) at a ratio of 1:50 α-SMA, 1:200 FAP, 1:200 Vimentin, 1:200 FSP-1, 1:00 PDGFRβ, and 1:100 PDGFRα for overnight at +4°C. Then, cells were washed with 1X PBS three times each 5 minutes intervals and incubated with the secondary antibody solution/PBS containing Alexa Fluor 488-conjugated goat anti-rabbit secondary antibody (#A11008, Life Technology) at 1:00, Alexa Fluor 647-conjugated phalloidin (#A22287, Life Technology) at 1:30 to stain actin filaments and DAPI at 1:1000 for 40 minutes at RT in dark environment. Finally, the coverslips were dipped into H2O once and mounted onto a slide using a mounting medium ((#50001, ibidi). The coverslips were then imaged under SP8 Confocal Microscopy (DMI8) and Zeiss Fluorescence Microscopy (HAL 100).

2.5.2. Staining for ccECM

To visualize ECM components of ccECM, we performed immunostaining for laminin and fibronectin. MDA-MB-231 cells were seeded onto coverslips at $5x10^4$cells/cm^2 and cultured for five days. After cells were removed using the freeze-thaw method, coverslips containing ccECM were exposed to 200U/ml DNAse-1 for 60 minutes at 37°C. Then, coverslips were fixed using 4% PFA. Fixed coverslips were blocked using 5% GS/PBS following the washing step with 1X PBS three times each at 5 minutes intervals. After blocking, coverslips were exposed to primary antibody/GS at 1:200 Laminin (Sigma # L9393) and 1:200 Fibronectin (Sigma, F3648) primary antibody overnight at +4°C. Coverslips were then incubated with secondary antibody/PBS conjugated with Alexa Fluor 488 goat-anti-rabbit secondary antibody at 1:200 and DAPI at 1:1000 for 40 minutes at RT and dark environment. In the final step, the coverslips were dipped into H2O and mounted on the slide using a mounting medium. The coverslips were imaged under SP8 Confocal Microcopy with 63X magnification using immersion oil.

2.6. Scanning Electron Microscopy (SEM)

We prepared the coverslips for SEM (Thermoscientific Quanta 250 FEG) microscopy to visualize whether decellularized coverslips harbor ccECM. For this, MDA-MB-231 cells were seeded onto coverslips coated with ITO, enabling electron transmission, at $50x10^5$ cells/cm^2 and cultured for five days. Then, coverslips were decellularized using either the freeze-thaw or the extraction buffer. Decellularized coverslips were fixed using prefixation solution containing 3% PFA and 1.5% glutaraldehyde (GA) for 2 hours in a laminar cabinet after treating 200U/ml DNAse-1 at 37°C. Fixed coverslips were washed with 1X PBS at 5 minutes intervals. We applied serial dehydration with different percentages of ethyl alcohol (EtOH) to remove water from washed coverslips completely. The coverslips were exposed to increased EtOH concentration with varying intervals of time; 50% for 5 minutes, 70% for 10 minutes, 80% for 10 minutes, 90% for 15 minutes, and 100% for 20 minutes in the laminar cabinet. Dehydrated coverslips were left in the laminar cabinet under air circulation until completely dried. Finally, dried coverslips were put into the desiccator until needed. The ccECM were imaged under SEM.

2.7. Qualitative Determination of ECM Proteins.

To determine ccECM proteins on decellularized coverslips, we used Coomassie blue staining. MDA-MB-231 cells were seeded on coverslips at $50x10^5$ cells/cm^2 and cultured for 3, 5, and 7 days. Then coverslips were decellularized using either the freeze-thaw or chemical solubilization method. Decellularized coverslips incubated with 0.1% Coomassie Blue solution containing 70% upH2O, 25% methanol, and 5% acetic acid for up to 30 minutes on a shaker. Then, the coverslips were dipped into the water once and allowed to completely dry.

2.8. Fabrication of Microfluidic Device

The microfluidic device, called Lab-on-a-chip (LOC), was produced using a 3D form lab printer. The mold was designed and printed by a 3D printer, and, after several washing steps with isopropyl alcohol, molds were ready to process. Polydimethylsiloxane (PDMS) and curing agent were mixed at a 1:10 ratio and poured over the molds. Then, PDMS was peeled out from molds and bonded to the glass surface via a UV/ozone crosslinker. LOC device consists of three channels which are the media channel (left), ccECM channel(right), and fibroblasts channel(middle). The middle channel is connected to left and right channels via two connectors, enabling cell migration for both sides.

2.9. Labeling of Fibroblasts

In migration assay, to track the fibroblasts green cell tracker (Cell tracker™ Green CMFDA dye, #C2925) was used. Briefly, before a day from seeding fibroblasts to the LOC device, they were washed with 1ml serum-free media. Then, the cell tracker was suspended in 1ml serum-free media, and the fibroblasts were exposed to 5μM of green tracker for 30 minutes at 37°C in a humidified incubator with 5% CO2. Once cells imported the dye, they were washed three times with 1ml serum-free media, and then their complete medium was added. They were checked under ZEISS fluorescence microscopy. Finally, green-stained fibroblasts were maintained at 37°C in a humidified incubator with 5% CO2 until needed.

2.10. Migration Assay

In order to observe the effect of ccECM on the fibroblasts' migration, we performed a day-dependent migration assay for four days. For migration assay, the LOC device was used (Figure 3.17A). Briefly, MDA-MB-231 cells were seeded on the upper channel at a $50x10^5$ cells/cm^2 ratio and cultured until reaching confluency. After four days from MDA-MB-231 seeding, the decellularization process was applied by the freeze-thaw method (2.2.2), and the LOC device was washed with 1X PBS, upH2O, and ethanol, respectively. The next step was seeding green-stained fibroblasts at $20,83x10^3$/cm^2 to the middle channel (Figure 3.17A). After the fibroblast attachment, all channels were filled with complete fibroblast media. Three hours(day0) after the green-stained fibroblast seeding, the cells were imaged by confocal microscopy with 10X magnification and tile scan option. The LOC device was observed for four days, including day0, and the migration capacity of the fibroblasts to both sides (3.17A) was assessed by ImageJ software.

2.11. Image Analysis

2.11.1. Quantification of Immunostaining Results

To quantify the fluorescence intensity of CAF markers, images were processed by ImageJ software. Firstly, images were exposed to subtraction after applying a Gaussian blur filter to eliminate the background. Then, the intensity of proteins was measured using the measure command and normalized to the cell numbers.

2.11.2. Quantification of Migration Analysis

Images were taken under confocal microscopy using a tile scan to measure the migration distance to see all regions. Then, the region of ınterst (ROI) was determined on brightfield images and fitted to fluorescence images following thresholding. We measured the XY coordinates of ROI as pixels for four days, and distance was normalized according to day0.

2.12. RNA Isolation and Q-RT PCR

For validation of proteins that were used for the characterization of CAFs, we performed q-RT-PCR. Briefly, MDA-MB-231 cells were seeded on 6 well plate with a specific cell number as indicated immunostaining section. Then, the freeze-thaw method was applied to obtain a surface with ccECM after 5 days of MDA-MB-231 cells seeding. Secondly, the fibroblasts were cultured on a decellularized 6 well plate containing ccECM and ccECM-free with or without 10ng/ml TGFβ treatment with specific cell counts indicated immunostaining section. After 48 hours of culture, the total RNA was extracted using PureLink® RNA Mini Kit (NucleospinRNA, #74095510) according to manufacturer procedure following flash freezing. cDNA was synthesized using the cDNA Synthesis Kit(ThermoScientifics, # K1622) from 1μg/ml RNA after the concentration of RNAs was measured by Nanodrop. To amplificate of desired genes, these cDNAs were processed in q-RT PCR using Essential DNA Green Master Mix (Roche, # 42729200) with 40 cycles on a Roche Real-Time PCR System. Cycle time(CT) values were normalized to the CT values of Tata-Box Binding Protein (TBP) to quantify desired genes. A formula indicated below was utilized to see fold changes.

Formula = $\mathbf{2^{-\Delta\Delta Ct} = 2^{\text{control group (target gene Ct value- TBP Ct value)-experimental group (target gene Ct value- TBP Ct value).}}}$

The cycles and primers used for q-RT PCR were summarized in tables 2.1 and 2.2, respectively.

Table 2.1. Cycles for q-RT PCR

Stage	Temperature	Duration	Cycle
Preincubation	95°C	600 s	1 cycle
3 step amplification	95°C	30 s	45 cycle
	60°C		
	72°C		
Melting	95°C	10 s	1 cycle
	65°C	60 s	
	72°C	1 s	

Table 2.2. Primers for q-RT PCR

Genes	Forward (5'---3') Primers	Reverse (5'---3') Primers
TBP	TAGAAGGCCTTGTGCTCACC	TCTGCTCTGACTTTAGCACCT
Vimentin	GCTAACCAACGACAAAGCCC	CGTTCAAGGTCAAGACGTGC
ACTA2/α-SMA	TCAATGTCCCAGCCATGTAT	CAGCACGATGCCAGTTGT
FAP	GAAAGAAAGGTGCCAATA	GATCAGTGCGTCCATCA
PDGFRβ	ACA CGG GAG AAT ACT TTT GC	GTT CCT CGG CAT CAT TAG GG
FSP-1/s100A4	TCCACAAGTACTCGGGCAAAG	CTCTTGGAAGTCCACCTCGT
CD29	CTGTGATGCCTTACATTAGCAC	ATCCAAATTTCCAGATATGCGC

2.13. Statistical Analysis

Unless otherwise stated, all data were analyzed by t-test(two-sample assuming unequal variances) to determine significance. The statistical indicator was taken as $p<0.05$, and data on the charts were reported as mean ± standard error. (otherwise, it was indicated in the figure legend).

CHAPTER 3.

RESULTS

3.1. SECTION I

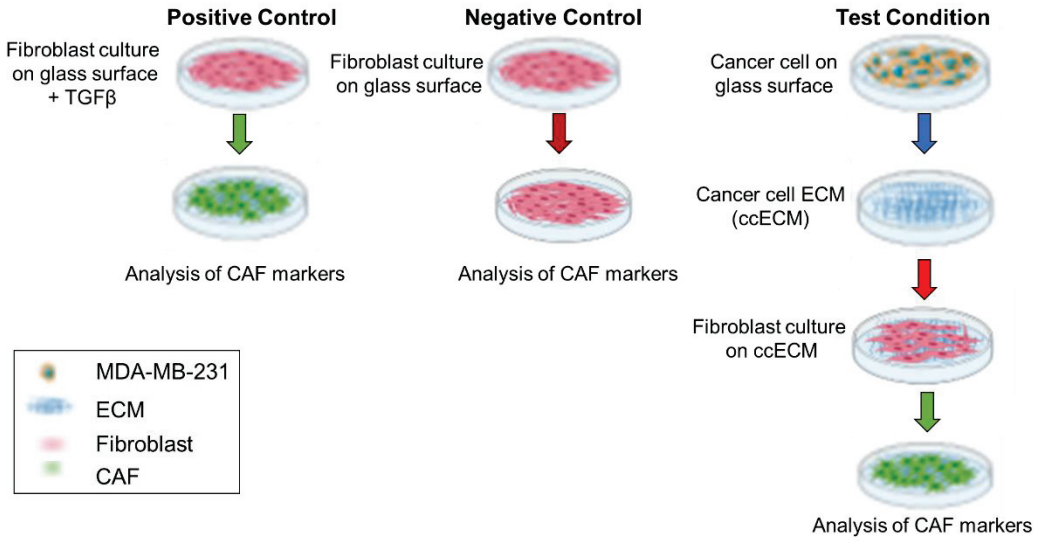

Figure 3. 1. Workflow of experimental design.

3.1.1. The Extraction Buffer was not able to Deposit ECM Components on the Surface After Decellularization

To verify that ccECM can be produced by cultured MDA-MB 231 cells, we first apply the extraction buffer method as in several studies[104, 106-108]. Coverslips were observed under light microscopy after decellularization by either the extraction buffer or the freeze-thaw on days 3, 5, and 7(Figure 3.2). Although a recent study utilizes ccECM from MDA-MB-231 cells using the extraction buffer method, they did not show any sign of ccECM on their paper[108]. Similarly, in our decellularized coverslips, we did not achieve to observe any indication of ccECM using the extraction buffer on days 3,5, and 7(Figure 3.2A). Due to the inability to produce ECM deposition with the extraction buffer, we sought new methods to get ccECM. As indicated in several works, the freeze-thaws

techniques could be used to create a cell-free scaffold from cell sheet[109, 110]. When coverslips were observed after decellularization by the freeze-thaw, there was something on those coverslips under light microscopy, which we called ccECM(Figure 3.2B).

3.1.2. ECM Depositions were Detectable Qualitatively with Coomassie Blue Staining

To determine whether decellularized coverslips had proteins, they were exposed to 0.1% coomassie blue dye in a dark place. Before staining decellularized coverslips, coomassie blue was tested using coverslips coated with 0.1mg/ml matrigel, and poly-L-lysine(PLL), and 0.05mg/ml collagen(Figure 3.3A). After checking of coomassie blue for qualitative determination of any protein on the surface, it was used for decellularized coverslips. When we performed that staining, there were no differences between the extraction buffer and the freeze-thaw method(Figure 3.3B).

Although there was no sign of ECM depositions on the coverslips decellularized by the extraction buffer(Figure 3.2A), coomassie blue staining indicated that both coverslip surfaces decellularized by the extraction buffer and the freeze-thaw had proteins (Figure 3.3B), which yielded a contradictory situation. Therefore, we proceeded with SEM to visualize those decellularized coverslips.

3.1.3. Decellularization of MDA-MB-231 Cells could Yield a Mesh Network by the Freeze-Thaw but not the Extraction Buffer

According to coomassie blue staining, both methods yielded ECM depositions on decellularized coverslips(Figure 3.3). However, we did not observe any deposits on the coverslips decellularized by the extraction buffer(Figure 3.2A). Hence we decided to visualize them under SEM in order to monitor whether those coverslips harbor any mesh network similar to decellularized ECM, as shown by Abigail C. Hielscher et al. in 2012[107]. Even though using the extraction buffer was not easy to handle ccECM from MDA-MB-231, they could observe the mesh network of ccECM only if they used the co-culture of a fibroblast cell line, having a high capacity to produce ECM depositions, with MDA-MB-231 under SEM.

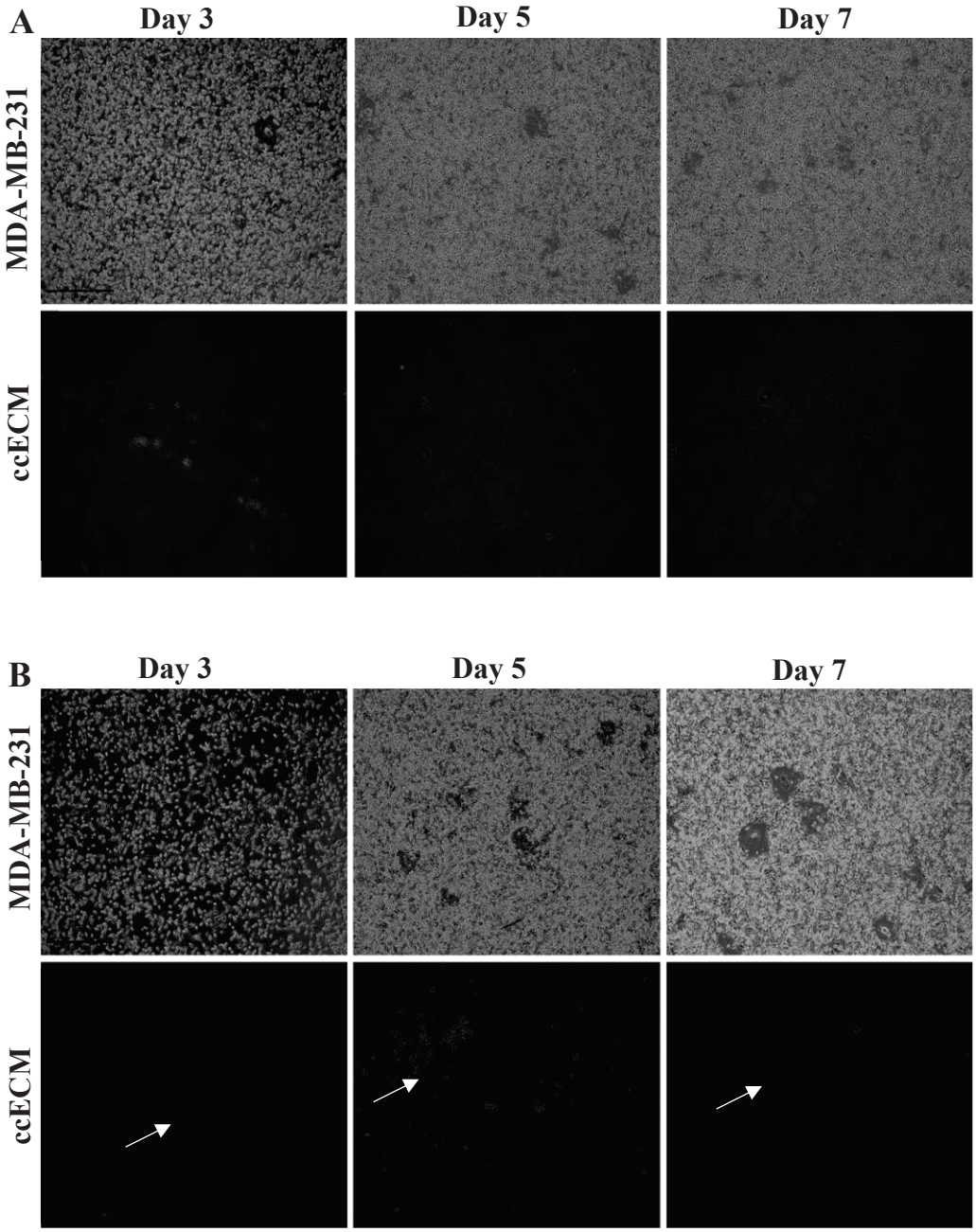

Figure 3.2. Decellularization of coverslips to verify ccECM coming from 3, 5, and 7 days cultured MDA-MB-231 cells. A. Decellarized coverslips(bottom) by the extraction buffer. B. Decullarized coverslips(bottom) by the freeze-thaw. Deposition of ccECMs were indicated by white arraows. Images were taken by light microscopy with . (Scale bar = 100μm)

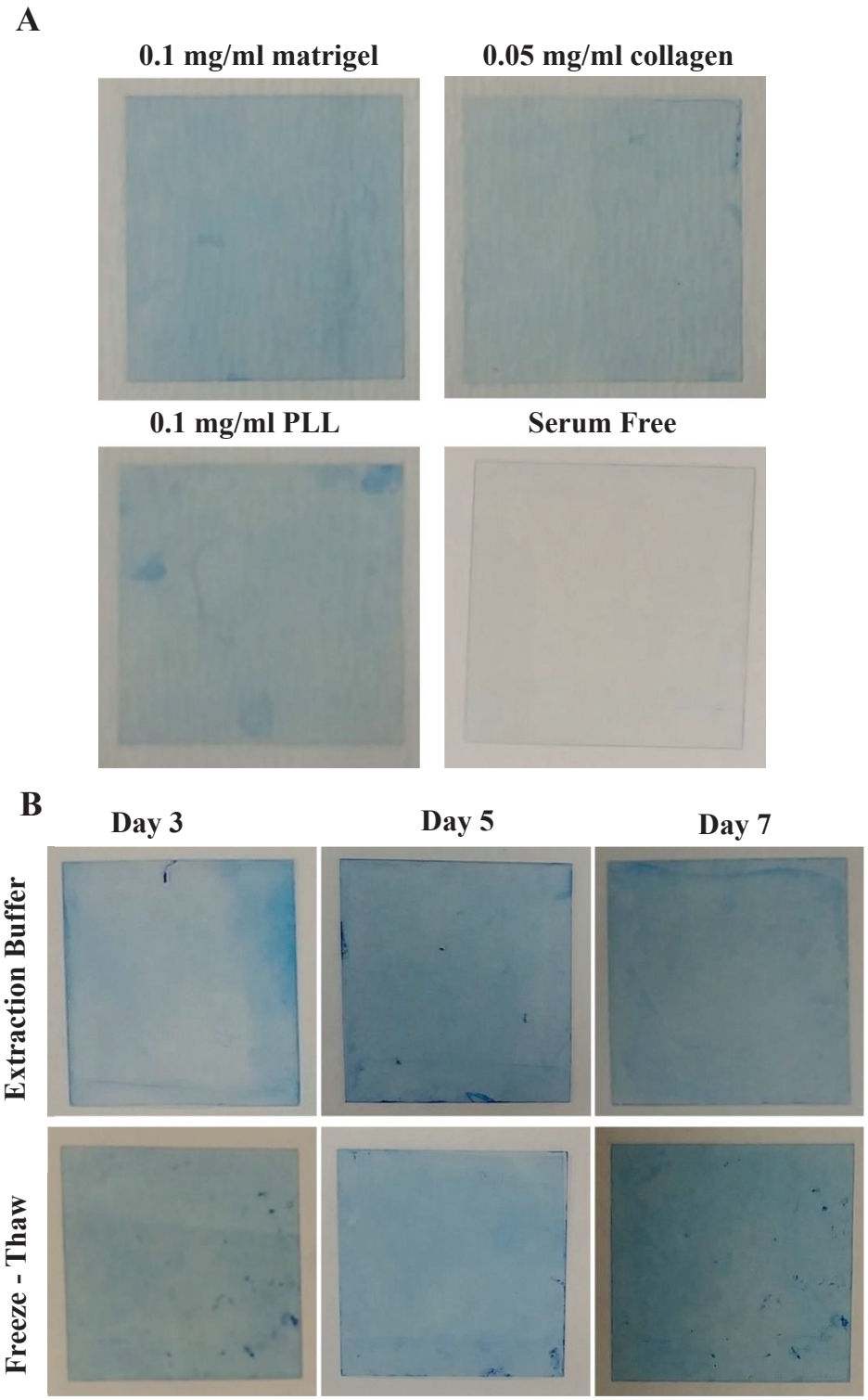

Figure 3.3. Staining of coverslips to qualitatively detect of ECM depositions. A. Testing of coomassie blue using different coating material. B. Qualitative determination of ECM deposition on coverslips decellularized either the extraction buffer(upper) or the freeze-thaw(bottom) on days 3, 5, and 7, respectively.

Consistent with their results, in our work, we observed a mesh network of ccECM on the coverslips decellularized from MDA-MB-231 cells by the freeze-thaw but not the extraction buffer on days 5 and 7(Figure 3.4). Since coverslips stained with coomassie blue indicated increased color and homogeneity on days 5 and 7(Figure 3.3B), we continued with those days for SEM(Figure 3.4). SEM results showed that decellularized coverslips by the freeze-thaw had a compact and network-like structure on day 5(Figure 3.4B).

In contrast, the coverslips decellularized by the extraction buffer had no proper structure (Figure 3.4A). Moreover, we also observed that the freeze-thaw method did not give a well-organized structure on day 7 (Figure 3.4B). To confirm the probability of obtaining ccECM on day 5, we repeat these experiments using DNAse treatment to rescue cell-free nuclei.

3.1.4. Decellularization of MDA-MB-231 Cells Left a Well-Organized Mesh Network by the Freeze-Thaw on Day 5

Since we observed ccECM on day 5, we repeated this experiment to check the reproducibility of conditions(Figure 3.5). We obtained similar results when comparing the coverslips decellularized by these two methods on day 5 (Figure 3.4, day 5). In the current setup, 200U/ml DNAse was applied to decellularized coverslips to eliminate any naked piece of DNA from ccECM[109](Figure 3.5). As indicated in that figure, DNAse treatment did not affect the mesh network of ccECM fibers when the freeze-thaw method was used (3.5A).

On the other hand, the extraction buffer still did not create useful ccECM for the incoming experiment (Figure 3.5B). Hence, we proceeded with the freeze-thaw method for further investigations.

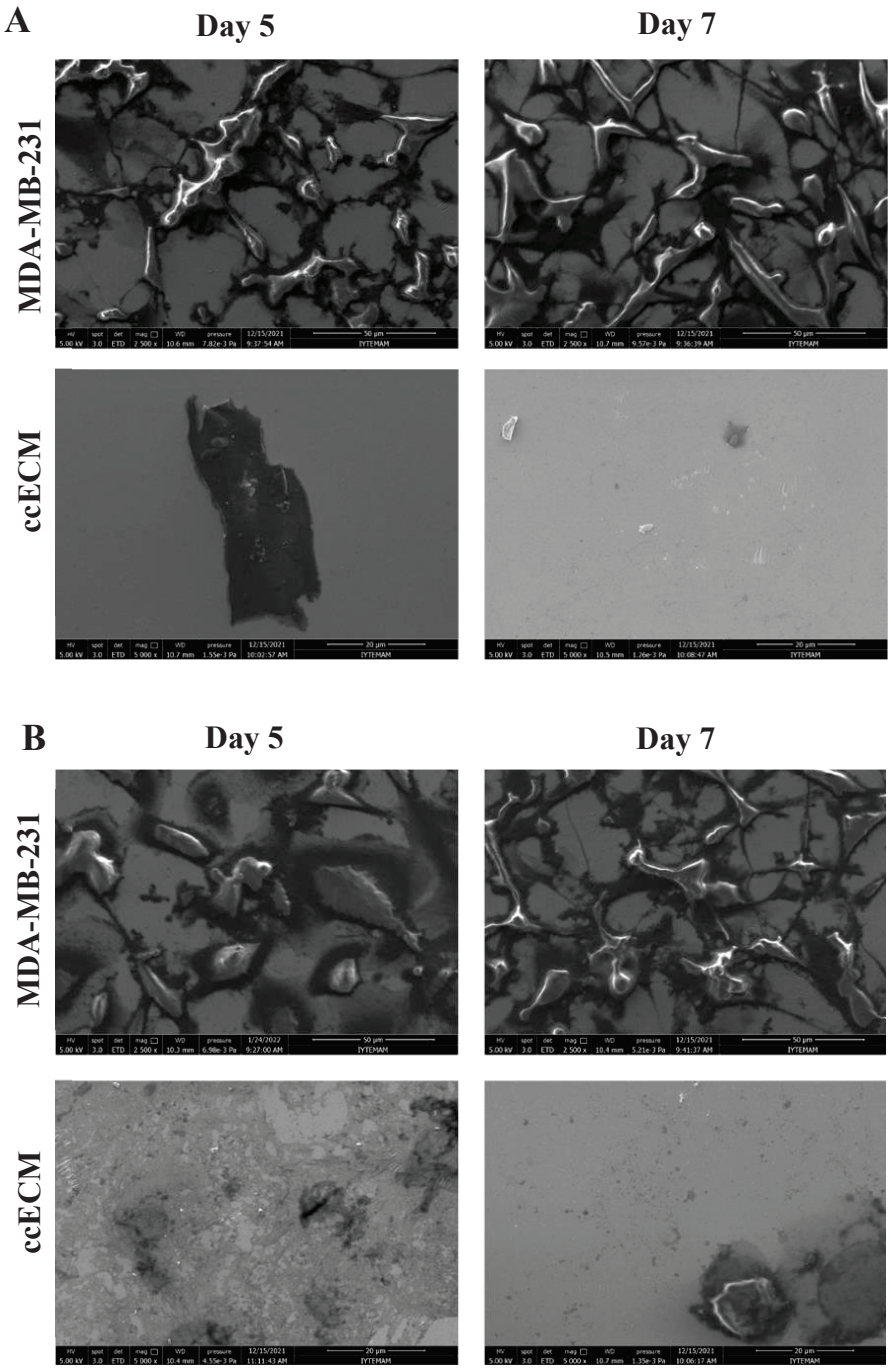

Figure 3.4. SEM verification of ccECM decellularized from MDA-MB-231 cells. A .Decellularized coverslips(bottom) by the extraction buffer on days 5 and 7. B. Decellularized coverslips(bottom) by the freeze-thaw on days 5 and 7. ccECM: MDA-MB-231 cell-derived extracellular matrix. Scale bar: 50µm for cells A, B upper, 20µm for ccECM A, B bottom.

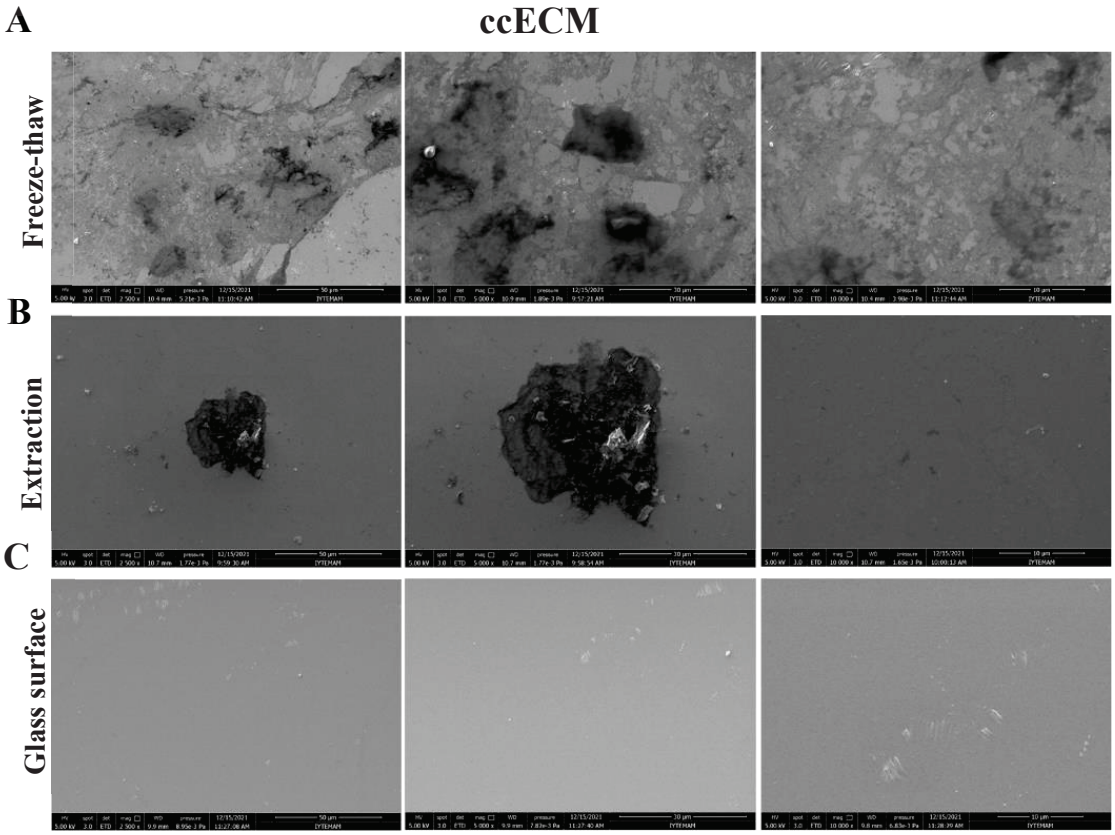

Figure 3.5. Comparison of ccECM on day 5 under SEM. A. Decellularized coverslips by the freeze-thaw. B. Decellularized coverslips by the extraction buffer. C. Glass surface for negative control. All surfaces were treated with 200U/ml DNAse. Scale bar: 50µm:30µ:10µm(from left to right)

3.2. SECTION II

3.2.1. DNAse Treatment of Coverslips Significantly Decreased The Naked DNA Remnant After Decellularization

After decellularization, DNA contamination might result from removing MDA-MB-231 cells from the surface, affecting downstream experiments when fibroblast is seeded on those ccECM. That is why we wanted to check whether there was any naked DNA on the decellularized surface using DAPI(Figure 3.6). Staining with DAPI showed that decellularized surface had free nuclei(Figure 3.6A). Before we progressed to downstream experiments, we wanted to ensure there was a cell nuclei-free surface after decellularization. Hence, decellularized surfaces were first treated with 100U/ml DNAse(Figure 3.6B, left). As seen in that figure, it also did not yield an acceptable nuclei-free surface. Decellularized surfaces were then exposed to 200U/ml DNAse as in other published studies[107, 109, 111]. Treating decellularized surfaces with 200U/ml DNAse eliminated the majority of free nuclei (Figure 3.6B, right). Thus, we progressed with 200U/ml DNAse treatment for each decellularized surface for future experiments.

3.2.2. Decellularized Surfaces Harbored Fibronectin And Laminin on Their Surface

To confirm that fiber-like structure was part of ECM, we conducted immunostaining upon fibronectin and laminin, which are physiologically present in ECM[107, 112, 113]. After culturing 5 days of MDA-MB-231 cells on the glass surface, it was decellularized by the freeze-thaw and treated with 200U/ml DNAse, and then they were processed through immunostaining. Here, we showed that decellularized surfaces had significantly increased expression of those ECM components (Figure 3.7). Figure 3.7A indicated that these ECM components were dispersed along the surface area. Compared to the glass surface, the decellularized surface had statistically increased intensity for fibronectin and laminin (Figure 3.7B), proving that the freeze-thaw method was useful for creating cell-free ECM from cultured cells. Therefore, we jumped to the next steps related to fibroblasts differentiation to CAFs using decellularized glass surface from 5 days of cultured MDA-MB-231 cells.

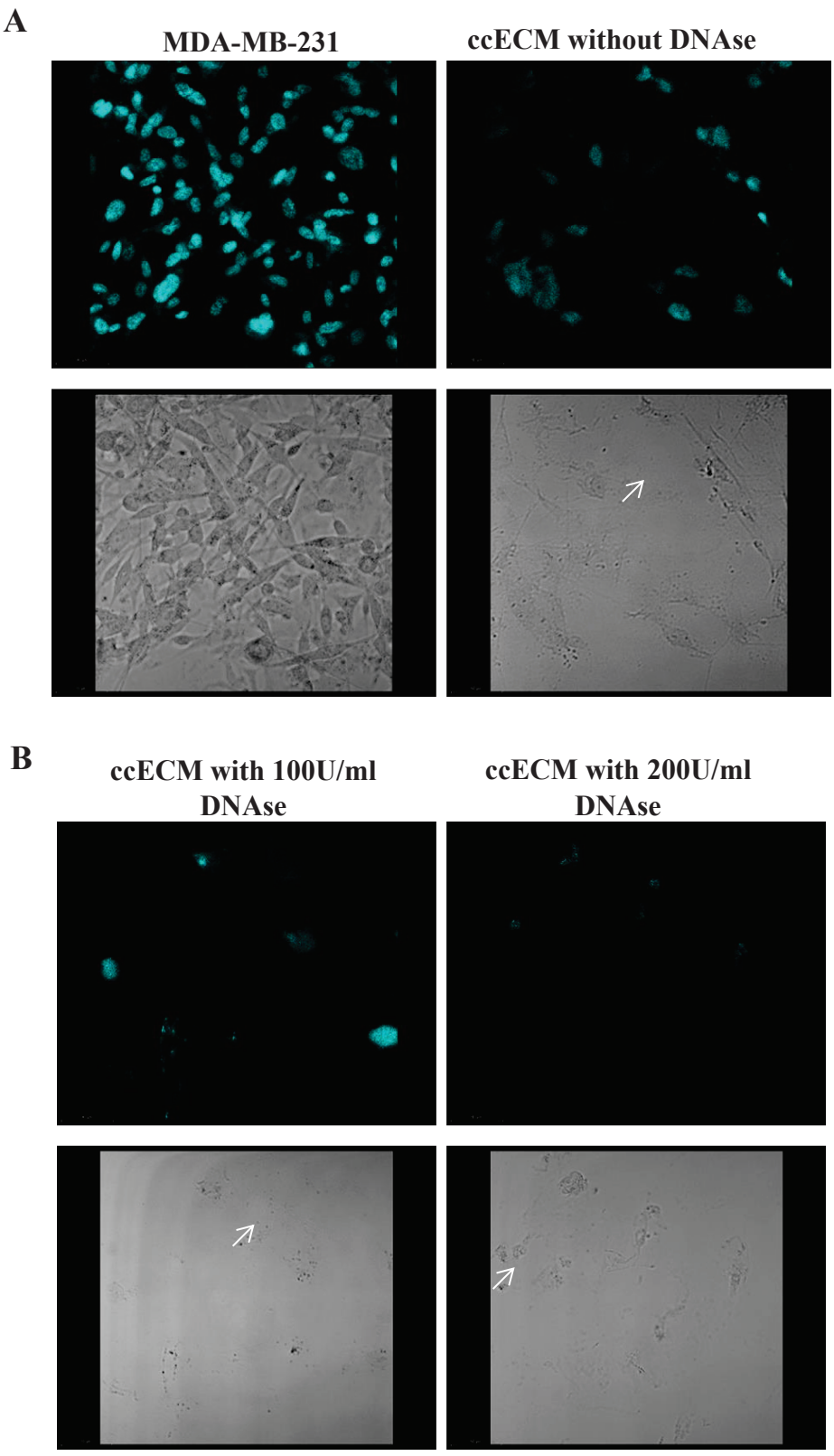

Figure 3.6. Elimination of free nuclei from decellularized surfaces using DNAse treatment. A. 5 days cultured MDA-MB-231 cells (left) and decellularized surface without DNAse treatment(right). B. Decellularized surface with

Figure 3.6-(cont) 100U/ml DNAse treatment(left) and 200U/ml DNAse treatment(right). Nuclei were stained with DAPI and indicated with blue color(upper). ECM depositions were indicated with white arrows in bright field images. Images were taken by confocal microscopy with 40x magnification. Scale bar: 50μm.

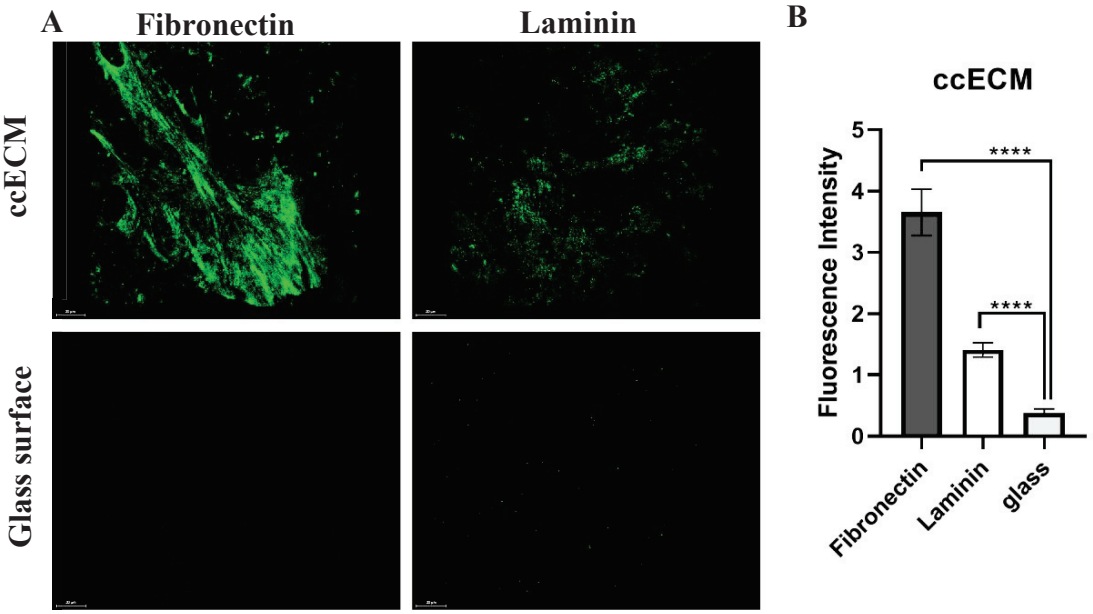

Figure 3.7. Confirmation of ECM components on decellularized ECM by immunostaining. A. Immunostaining for fibronectin on ccECM versus glass surface(left) and laminin versus glass surface(right). B. Fluorescence intensity of fibronectin, laminin on decellularized and glass surface (n=3; p< 0.0001; ****). Images were taken by confocal microscopy with 63X magnification using immersion oil. (Scale bar: 20μm). Statistical analysis was performed using unpaired t test (* p<0,05; ** p<0,01; *** p<0,005 ; **** p< 0,0001). The error bars represent the standard error.

3.3. SECTION III

ccECM Facilitated The Differentiation of Fibroblast to Cancer-Associated Fibroblast

To understand whether the decellularized ccECM facilitated fibroblast differentiation to CAFs, fibroblast cell line, W1-38, was cultured onto those ccECM for 48 hours. Although there are debating issues regarding activation of fibroblast, a common cytokine called TGFβ induces fibroblast in both autocrine and paracrine[74, 75, 78, 80]. Hence, we used 10ng/ml TGFβ as a positive control in our experimental setup. Another problem arises when one wants to identify CAFs since no such marker could be used to characterize them. Indeed there are several markers, including vimentin, FAP, PDGFRβ, α-SMA, and FSP-1/s100A4[114, 115]. Therefore we included those markers in determining whether fibroblast on ccECM differentiated to CAFs.

3.3.1. Fibroblast on ccECM Showed a Significant Increase in Vimentin Expression at the Protein Level but not mRNA Level

One of our markers was vimentin which is a type III intermediate filament. Vimentin is generally located at different places on the cells but is mainly present in the cytoplasm and membrane. It participates variety of cellular events such as cell regulation, maintenance of mechanotransduction, and prevention of mechanical stress[116]. Here, we found that vimentin expression in TGFβ-induced fibroblast was much greater than fibroblast on the glass surface (Figure 3.8A, 3.8B, n=3, **** $p < 0.0001$), which indicated TGFβ induced fibroblast activation. Consistently, vimentin expression increased when it cultured on ccECM compared to glass surface (3.8A, 3.8B, n=3, ****$p < 0.0001$). We did not observe any differences between TGFβ-induced fibroblast and fibroblast on ccECM(Figure3.8B, n=3, ns). Next, we wanted to validate our immunostaining results by performing RT-PCR upon CAFs markers.

Contrary to immunostaining results, none of our conditions showed significant vimentin expression compared to control (3.8C). According to our data, fibroblast on ccECM indicated 32% (Figure 3.6C, n=3, ns) and 11%(Figure 3.6C, n=3, ns) decrease expression

compared to control and TGFβ treated cells, respectively. On top of it, TGFβ-induced cells were also decreased by 16% more than the control group (Figure 3.6C, n=3, ns).

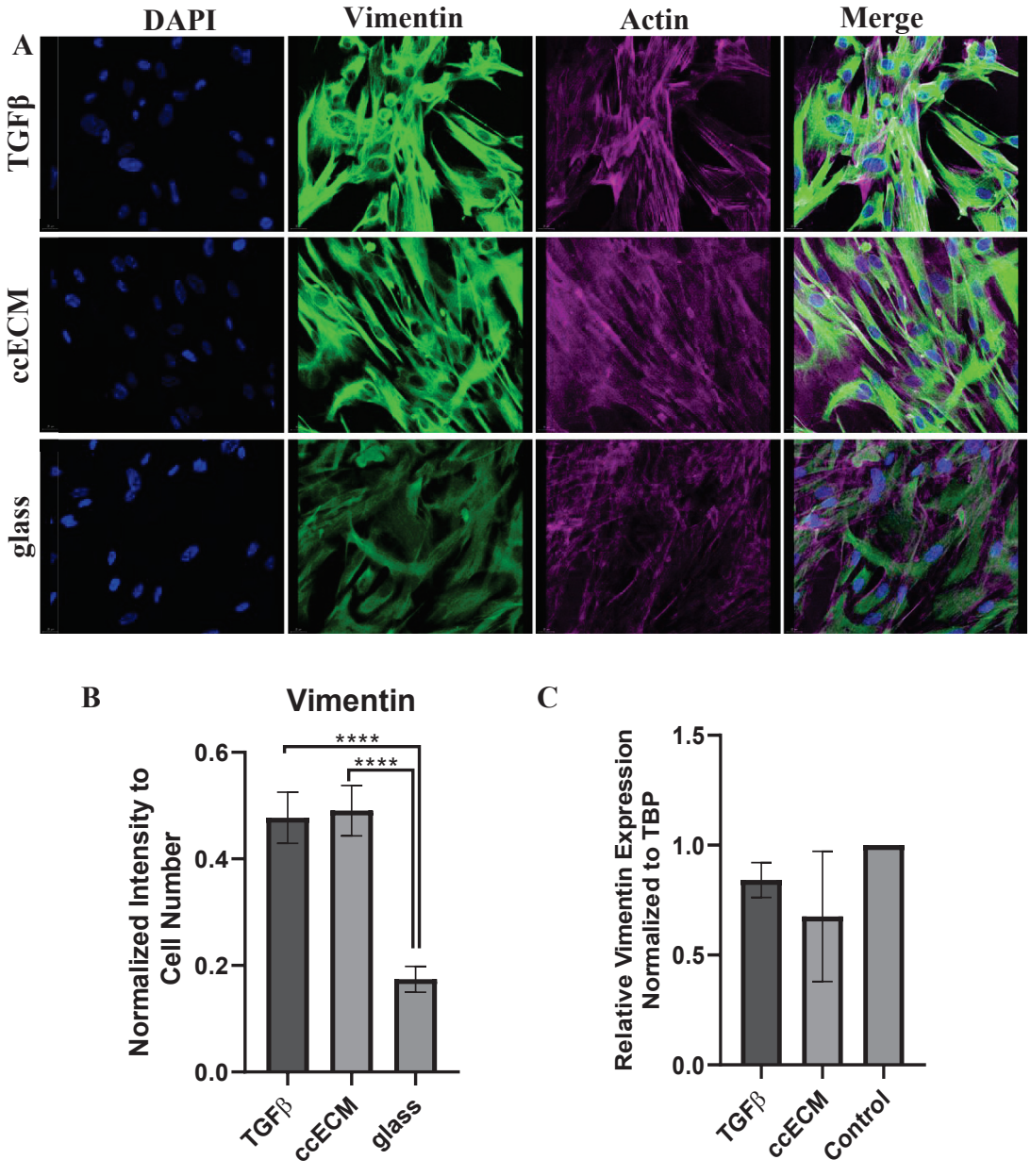

Figure 3.8. Vimentin expression on fibroblast cultured on ccECM for 48 hours. A. Immunostaining for vimentin in fibroblast ınduced with 10ng/ml TGFβ(upper), cultured on decellularized ccECM(middle), and cultured on the glass surface(bottom). Images were taken by confocal microscopy with 40X magnification. Cell nuclei were stained with DAPI and represented with blue(1st line), vimentin intensity was represented with green(2nd line), and actin was stained with Alexa Fluor 647 conjugated phalloidin and represented with magenta(3rd

Figure 3.8-(cont) line). Scale bar: 20μm. B. Green intensity for vimentin normalized to cell number(n=3; p< 0.0001; ****) C. Relative mRNA expression of vimentin normalized to TBP(n=3). Statistical analysis was performed using unpaired t test (* p<0,05; ** p<0,01; *** p<0,005 ; **** p< 0,0001). The error bars represent the standard error.

3.3.2. Fibroblast on ccECM Showed Significant Increased FAP Expression at the Protein Level But was not Significant at the mRNA Level

Our second marker was one type II serin protease called FAP, located at cell surface[117]. It is also one of the strong markers for characterizing of CAFs. In addition to vimentin, we checked FAP on both protein and mRNA levels. According to our immunostaining experiment results, FAP was significantly increased in fibroblast when they cultured on ccECM(Figure 3.9A, 3.9B, n=2, ****p< 0.00001) and induced with TGFβ(Figure 3.9A, 3.9B, n=2, ****p< 0.00001) compared to fibroblast in glass surface. While there were no differences between ccECM and TGFβ groups in vimentin(Figure3.8B, n=2), FAP expression was also significantly increased in fibroblast activated with TGFβ(Figure3.9B, n=2, *** p<0.005) than fibroblast on ccECM. mRNA levels of FAP, on the other hand, showed an inverse correlation (Figure3.9C). It was decreased 45% (Figure 3.9C, n=3, ns), 72% (Figure 3.9C, n=3, ** p<0.01) compared to control and TGFβ group, respectively. As expected, TGFβ-induced fibroblast was 2,5 fold greater than the control group (Figure 3.9C, n=3, * p< 0.05).

3.3.3. PDGFRβ Protein Level Showed an Increased Trend in Fibroblast Cultured on ccECM

Another marker for the identification of CAF is PDGFRβ. It is one of the type III tyrosine-protein kinase receptors on cell surface[118]. When we stained for PDGFRβ by immunostaining, we observed that fibroblast on ccECM had boosted expression than fibroblast on the glass surface(Figure 3.10B, n=2, ** p<0.01) and cells treated with TGFβ (Figure3.10B, n=2, ** p<0.01).

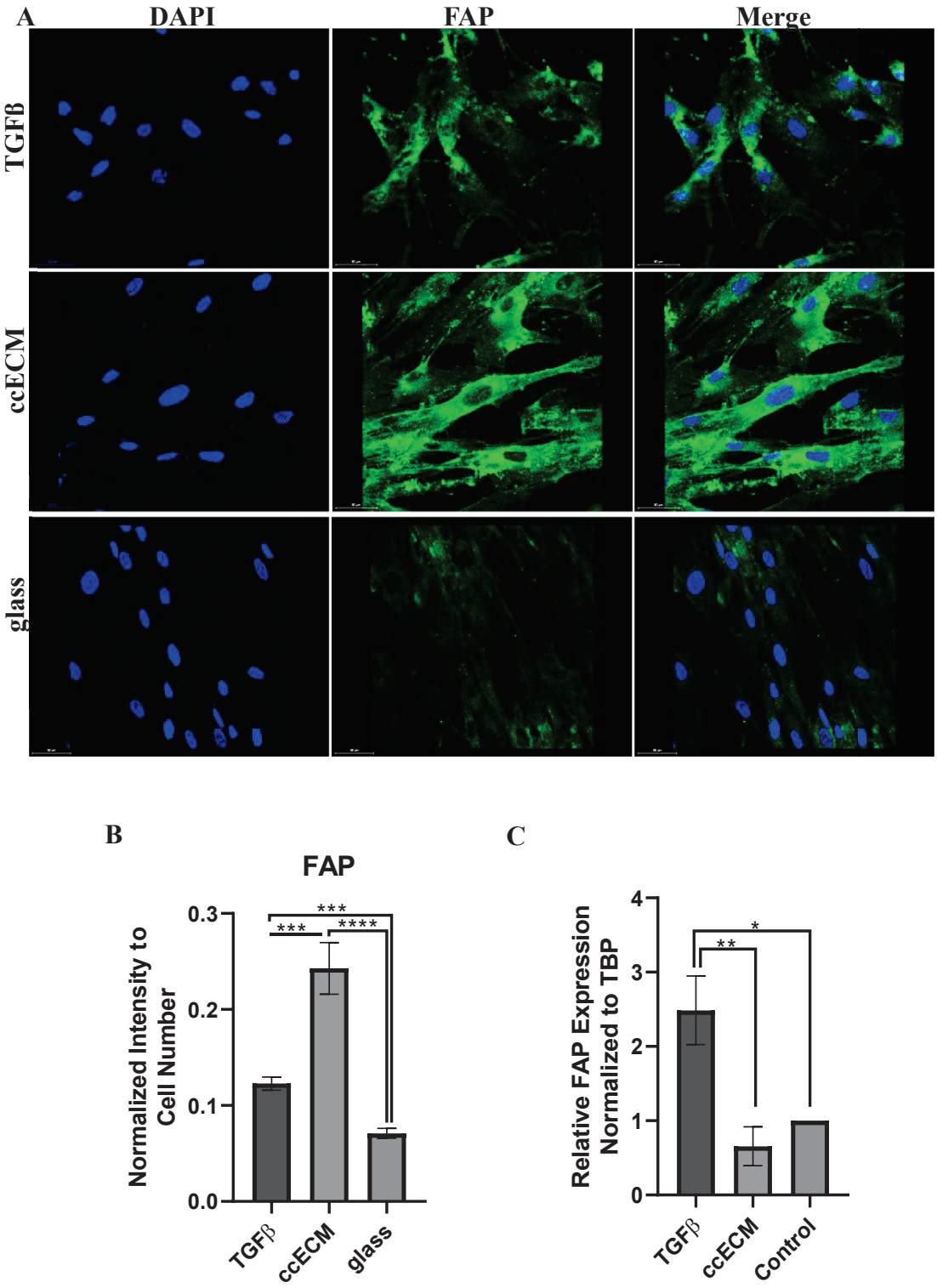

Figure 3.9. FAP expression in fibroblast cultured on ccECM for 48hours. A. Immunostaining upon FAP in fibroblast induced with 10ng/ml TGFβ (upper), cultured on decellularized ccECM(middle), and cultured on the glass surface(bottom). Images were taken by confocal microscopy with 40X magnification. Cell nuclei were stained with DAPI and represented with blue (1st line), FAP intensity was represented with green(2nd line),

Figure 3.9-(cont) and channels were merged(3rd line). Scale bar: 20μm. B. Green intensity for FAP normalized to cell number. C. Relative mRNA expression of FAP normalized to TBP(n=3). Statistical analysis was performed using unpaired t test (* p<0,05; ** p<0,01; *** p<0,005 ; **** p< 0,0001). The error bars represent the standard error.

Besides PDGFRβ expression in fibroblast cultured on ccECM, fibroblast induced with TGFβ showed a significant increase(Figure 3.10B, n=2, * p<0.05) compared to fibroblast on the glass surface. Unlike immunostaining results, mRNA expression levels indicated fibroblast on ccECM showed a 25%(Figure 3.10C, n=3, ns) and 40%(Figure 3.10C, n=3, ns) decrease trend than the control group(Figure 3.10C). Dissimilar to the relative mRNA level of PDGFRb in fibroblast cultured on ccECM, data showed that the cells induced by TGFβ were 1,3 fold greater than the control group(Figure 3.10C, n=3, ns).

3.3.4. α-SMA did not Show a Significant Increase in Fibroblast Cultured on Decellularized ECM

Our next marker is α-SMA, the one 6 isoforms of mammalian actin family[45]. It is an intermediate filament-associated protein within cells and is expressed in several cell types, including activated fibroblast[40, 119]. Since it is also a common marker for CAFs identification, we included it in our dataset. However, as indicated in Figures 3.11B and 3.11C, α-SMA did not show a significant correlation according to immunostaining results. (Figure 3.11A). There were only differences between TGFβ-induced cells and fibroblast on ccECM(Figure 3.11B, n=1, * p<0.05). Even RT-PCR results revealed that α-SMA expression on ccECM cultured fibroblast indicated an 18%(Figure 3.11C, n=3, ns) and 86%(Figure 3.11C, n=3, ns) decrease compared to control and fibroblasts activated with TGFβ, respectively. Interestingly, there was a dramatic decrease in fibroblast cultured on ccECM(Figure 3.11C, ns) than TGFβ induced cells.

3.3.5. FSP1 did not Change at The Protein Level in Fibroblasts Cultured on ccECM

FSP1 is a fibroblast-specific filament-associated protein belonging to the s100 cytoplasmic calcium binding protein family, located at the cell nuclei, cytoplasm, and

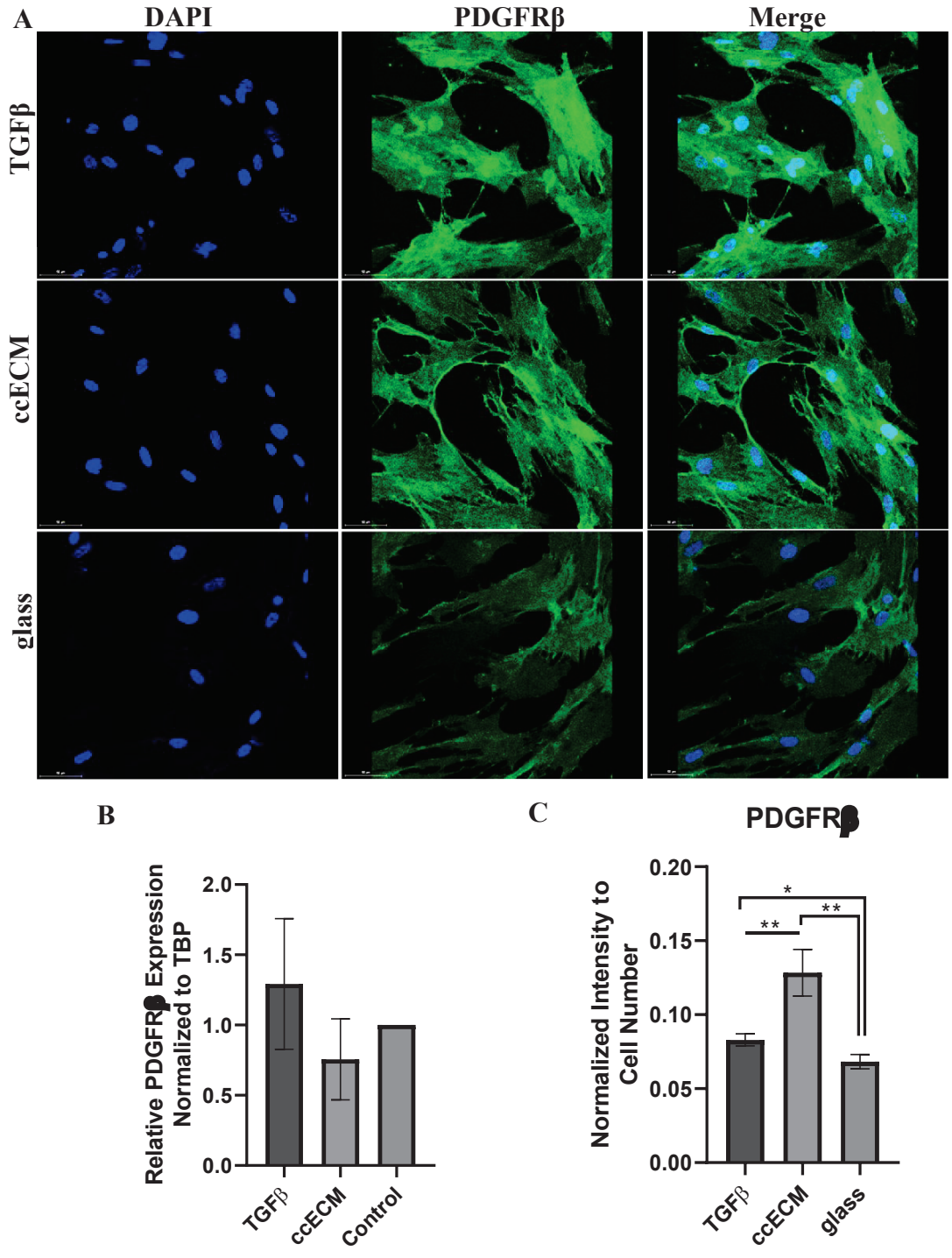

Figure 3.10. PDGFRβ expression in fibroblast cultured on ccECM for 48 hours. A. Immunostaining for PDGFRβ in fibroblast induced with 10ng/ml TGFβ(upper), cultured on decellularized ccECM(middle), and cultured on the glass surface(bottom). Images were taken by confocal microscopy with 40X magnification. Cell nuclei were stained with DAPI and represented with blue (1st line), PDGFRβ intensity was represented with green(2nd line), and channels were merged(3rd line). Scale bar: 50μm. B. Green intensity for PDGFRβ normalized to cell number(n=2). C. Relative mRNA expression of PDGFRβ normalized to TBP(n=3). Statistical analysis was performed using unpaired t test (* p<0,05; ** p<0,01; *** p<0,005 ; **** p< 0,0001). The error bars represent the standard error.

ECM[120]. Hence, it is one of the markers used if one wants to characterize fibroblast and CAFs[121]. Based on our immunostaining results, its expression did not differ compared to TGFβ induced cells(Figure 3.12B, n=3, ns) and fibroblast on the glass surface(Figure 3.12B, n=3, ns). However, figure 3.12C indicated that the relative expression of FSP1 in the ccECM group was 1.07(n=3, ns) and 3.35(n=3, * p<0.05) fold greater than the control and TGFβ condition, respectively.(Figure 3.12C, n=3). Inversely, cells treated with 10ng/ml TGFβ showed 68% decrease expression of FSP1 compared to control(Figure 3.12C,n=3, *** p<0.005).

3.3.6. ccECM Decreased the Relative Expression of CD29 in Fibroblast

CD29, also known as integrin beta-1 (ITGB1), is another marker thanks to its clinical importance in identifying tumors and CAFs as well[65]. As indicated in Figure 3.13, relative mRNA expression of CD29 showed a 16%(n=3, ns) and 54%(n=3, * p<0.05) decrease when compared to control and TGFβ treated groups. Although TGFβ-induced cells had 1.82 fold greater expression than the control, it was not statistically significant.(Figure 3.13, n=3, ns).

3.3.7. Fibroblast Cultured on ccECM Showed a Decrease in Fibronectin Intensity

One of the main components of ECM, fibronectin, is a type of glycoproteins that provides the bridge between the inside and outside of cells interacting with integrins[122].

Hence, we considered its intensity after the fibroblasts had been cultured on ccECM. According to our results, fibronectin intensity in fibroblast cultured on ccECM decreased compared to the fibroblast on the glass surface(Figure 3.14B, n=3, ns), and the fibroblasts activated by TGFβ(Figure 3.14B, n=3, ** $p<0.01$). While fibronectin was slightly increased in TGFβ treated fibroblasts than in the control group (Figure 3.14B, n=3, ns).

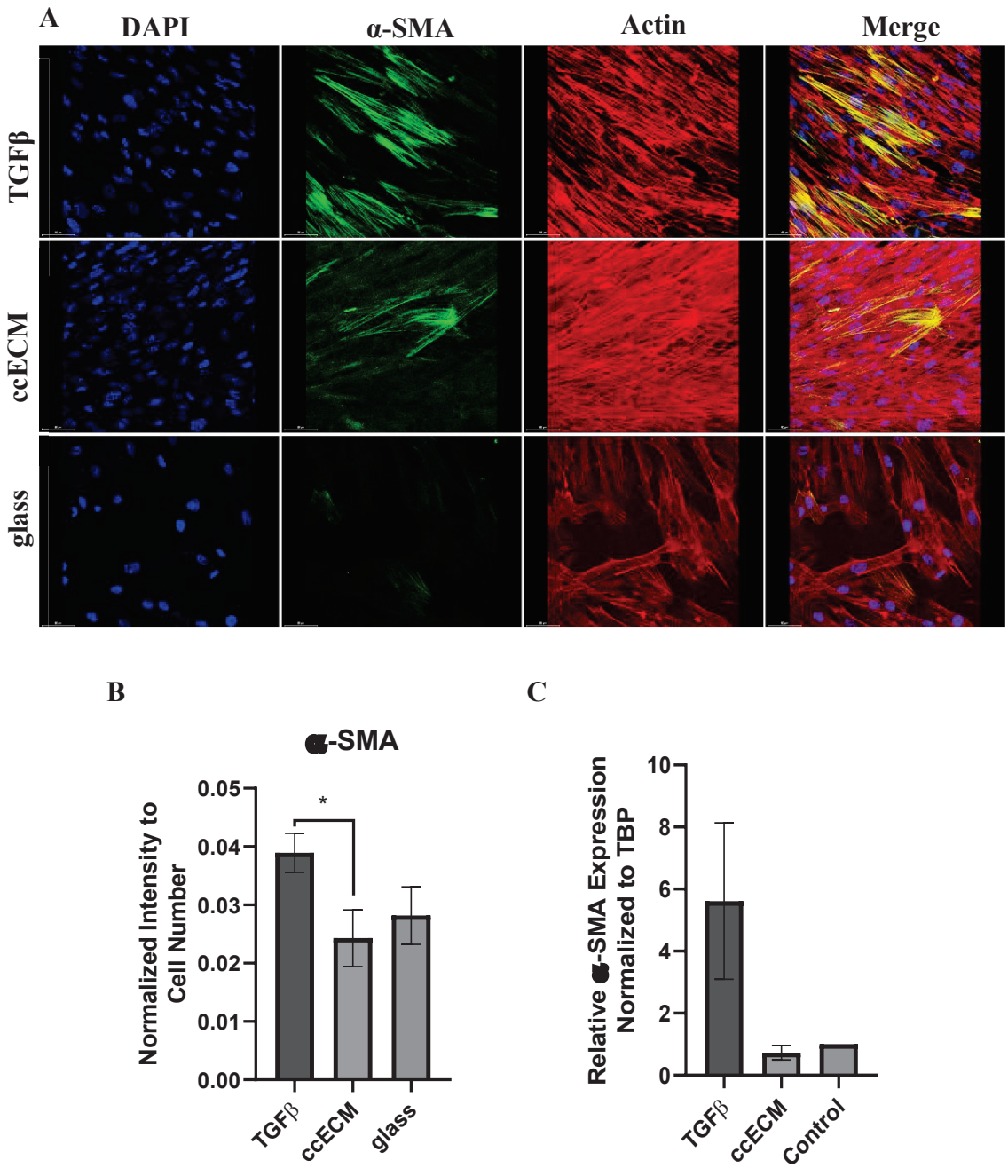

Figure 3.11 α-SMA expression on fibroblast cultured on ccECM for 48 hours. A. Immunostaining for α-SMA in fibroblast ınduced with 10ng/ml TGFβ(upper), and cultured on decellularized ccECM(middle), and cultured on the glass surface(bottom). Images were taken by confocal

Figure 3.11–(cont) microscopy with 40X magnification. Cell nuclei were stained with DAPI and represented with blue(1st line), α-SMA intensity was represented with green(2nd line), and actin was stained with Alexa Fluor 5555 conjugated phalloidin and represented with red(3rd line). Scale bar: 50μm. B. Green intensity for α-SMA normalized to cell number(n=1) C. Relative mRNA expression of α-SMA normalized to TBP(n=3). Statistical analysis was performed using unpaired t-test (* p<0,05; ** p<0,01; *** p<0,005 ; **** p< 0,0001). The error bars represent the standard error.

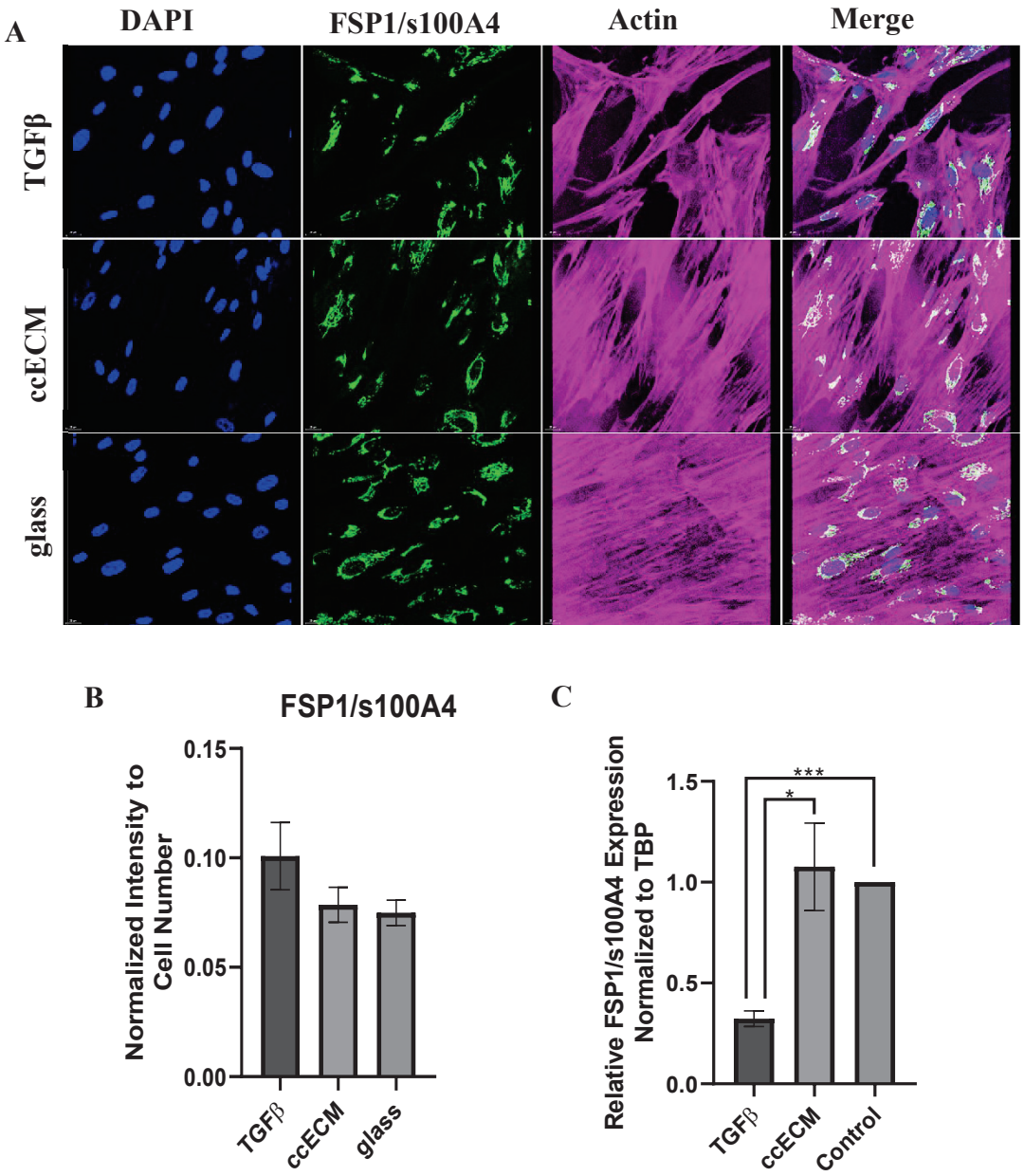

Figure 3.12. FSP1 expression on fibroblast cultured on ccECM for 48 hours. A. Immunostaining for FSP1 in fibroblast ınduced with 10ng/ml TGFβ(upper), cultured on decellularized ccECM(middle), and

Figure 3.12- (cont) cultured on the glass surface(bottom). Images were taken by confocal microscopy with 40X magnification. Cell nuclei were stained with DAPI and represented with blue(1st line), FSP1 intensity was represented with green(2nd line), and actin was stained with Alexa Fluor 647 conjugated phalloidin and represented with magenta(3rd line). Scale bar: 20μm. B. Green intensity for FSP1 normalized to cell number(n=3) C. Relative mRNA expression of FSP1 normalized to TBP(n=3). Statistical analysis was performed using unpaired t-test (* p<0,05; ** p<0,01; *** p<0,005 ; **** p< 0,0001). The error bars represent the standard error

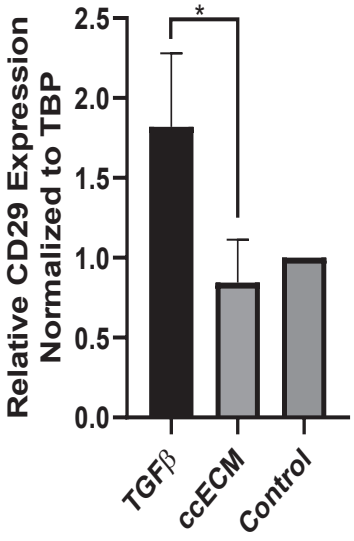

Figure 3.13. Relative mRNA expression of CD29 in fibroblast cultured on ccECM for 48 hours. CD29 expression was normalized to TBP(n=3, ns). Statistical analysis was performed using unpaired t test (* p<0,05; ** p<0,01; *** p<0,005 ; **** p< 0,0001). The error bars represent the standard error.

3.3.8. Fibroblast Cultured on ccECM Showed a Decreased Laminin Intensity

The last marker we investigated is laminin, a type of glycoprotein in ECM that provides signaling transduction working with plasma membrane-anchored receptor[123]. Based on our immunostaining results, laminin intensity was significantly decrease in fibroblasts cultured on ccECM than control(Figure 3.15B, n=3, *** p< 0.001) and TGFβ treated fibroblasts(Figure 3.15B, n=3, *** p< 0.001). Unlike ccECM, TGFβ-treated

fibroblast did not show significant changes than the control group (Figure 3.15B, n=3, ns).

3.3.9. ccECM Affected the Attachment of the Fibroblasts

During our immunostaining and mRNA experiments, we realized that ccECM affected fibroblast differentiation and increased cell proliferation when the fibroblast was cultured on decellularized ccECM (Figure 3.16A). As it was represented in bright field images, fibroblasts cultured on ccECM showed better attachment within 2 and 6 hours (Figure 3.16, 2nd line). In order to quantify them, we utilized DAPI staining after 48 hours from fibroblast cultured on ccECM (Figure 3.16B).

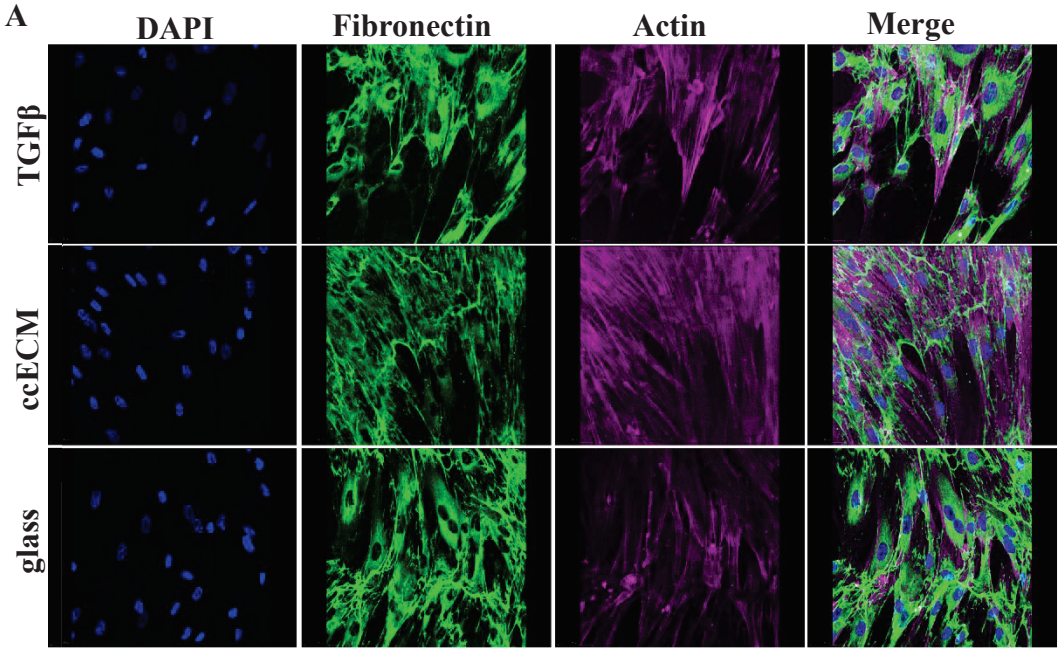

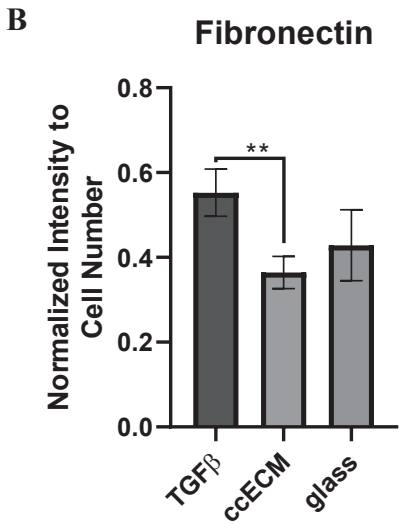

Figure 3.14. Fibronectin intensity decreased when the fibroblast was cultured on ccECM for 48 hours. A. Immunostaining for fibronectin in fibroblast induced with 10ng/ml TGFβ(upper), cultured on decellularized ccECM(middle), and cultured on the glass surface(bottom). Images were taken by confocal microscopy with 40X magnification. Cell nuclei were stained with DAPI and represented with blue(1st line), fibronectin intensity was represented with green(2nd line), actin was stained with Alexa Fluor 647 F conjugated phalloidin and represented with magenta(3rd line). Scale bar: 50µm B. Green intensity for Fibronectin normalized to cell number(n=3). Statistical analysis was performed using unpaired t-test (* p<0,05; ** p<0,01; *** p<0,005 ; **** p< 0,0001). The error bars represent the standard error

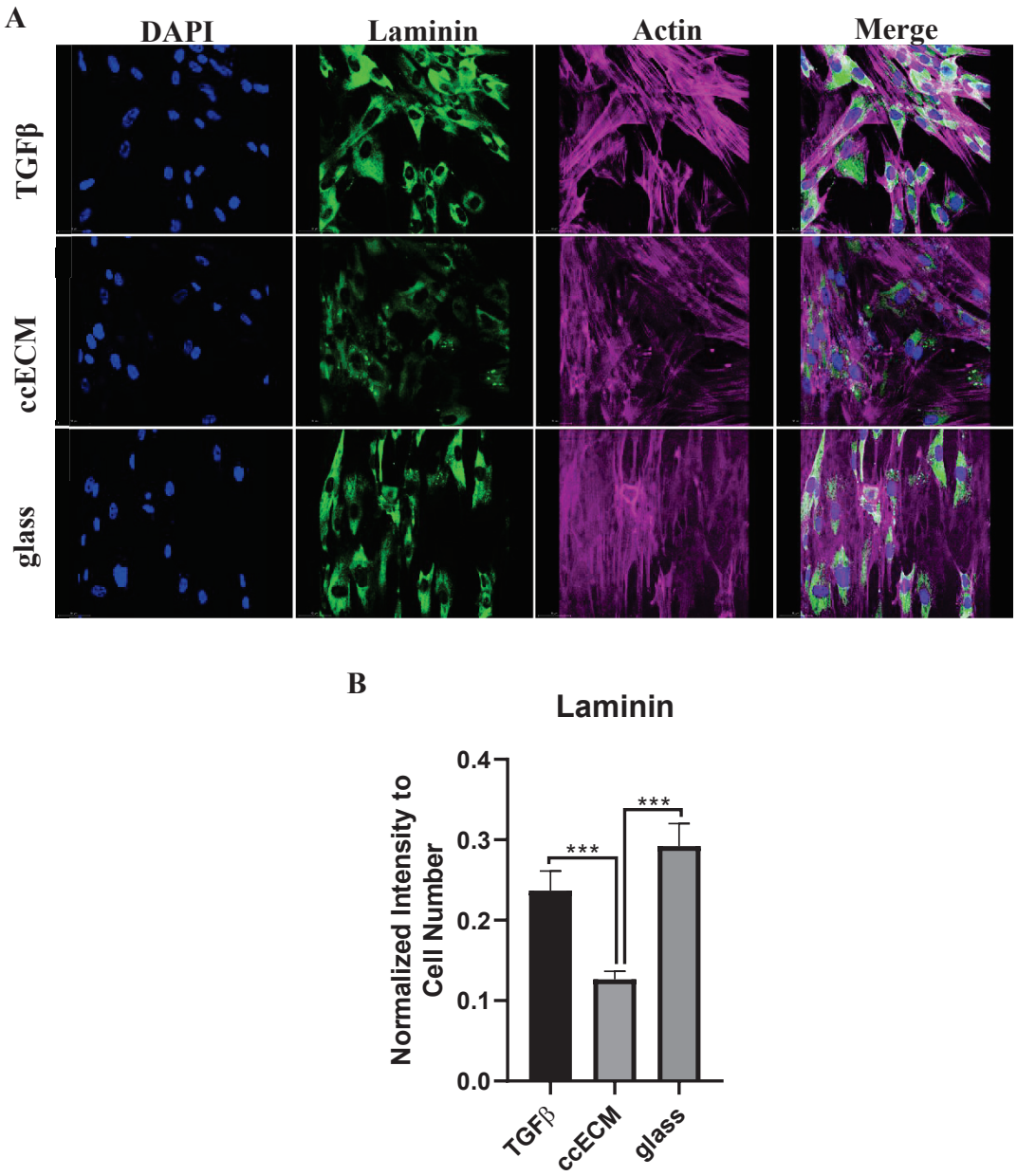

Figure 3.15. Laminin intensity decreased when the fibroblast was cultured on ccECM for 48 hours. A. Immunostaining for laminin in fibroblast induced with 10ng/ml TGFβ(upper), cultured on decellularized ccECM(middle), and cultured on the glass surface(bottom). Images were taken by confocal microscopy with 40X magnification. Cell nuclei were stained with DAPI and represented with blue(1st line), laminin intensity was represented with green(2nd line), and actin was stained with Alexa Fluor 647 conjugated phalloidin and represented with magenta(3rd line). Scale bar: 50μm B. Green intensity for laminin normalized to cell number(n=3). Statistical analysis was performed using unpaired t-test (* p<0,05; ** p<0,01; *** p<0,005 ; **** p< 0,0001). The error bars represent the standard error.

Moreover, we included our immunostaining datasets to extend the number of biological repeats. DAPI stained coverslips were collected and made stack using ImageJ software. After applying a gaissum blur filter to eliminate background noise, they were substracted, and finally, we obtained images that were able to count in that software (Figure

B). Later on, each DAPI point was counted for all conditions using analyzed particles. Similar to bright-field images (Figure 3.16A), fibroblasts cultured on ccECM for 48 hours showed significantly higher cell numbers compared to TGFβ treated cells and control (Figure 3.16C, n=8, *** p<0.005). Unlike ccECM, TGFβ did not change fibroblasts cell numbers compared to control (Figure 3.16C, n=8, ns).

3.3.10. ccECM did not Show a Significant Effect on the Migration of Fibroblast

In addition to the effect of ccECM on the differentiation of fibroblasts, as another approach, we tested whether ccECM was able to recruit fibroblasts to their site. To perform that, we used a LOC device which allowed us to do multiple experiments simultaneously. This system contains three separated channels connected with two connectors that allow cells to migrate (Figure 3.17A). To create ccECM, MDA-MB-231 cells were cultured on the right channel until reaching 100% of confluency (4 days), and then cells were removed using the freeze-thaw. After decellularization, green-stained fibroblasts cells were seeded on the middle channel and allowed to migrate horizontally. Their migration capacity was imaged by confocal microscopy for four days. The distance

of fibroblast from the start line to the ccECM channel (white array) or ccECM free channel (black array) was measured depending on the days to interpret the results.

Based on our results, after 3 hours from the seeding of the fibroblast (Figure 3.17A), they were an attempt to migrate to the ccECM side(Figure 3.17B, n=3, * $p<0.05$). Although the fibroblast migrated to the ccECM side more than the control (Figure 3.17C), this situation disappeared as time passed (Figure 3.17D, n=3, ns). In figure 3.17E, we indicated the fibroblast's migration towards both sides represented with different pseudocolors in a day-dependent manner. (red:day0, green:day1, blue:day2, and magenta:day3).

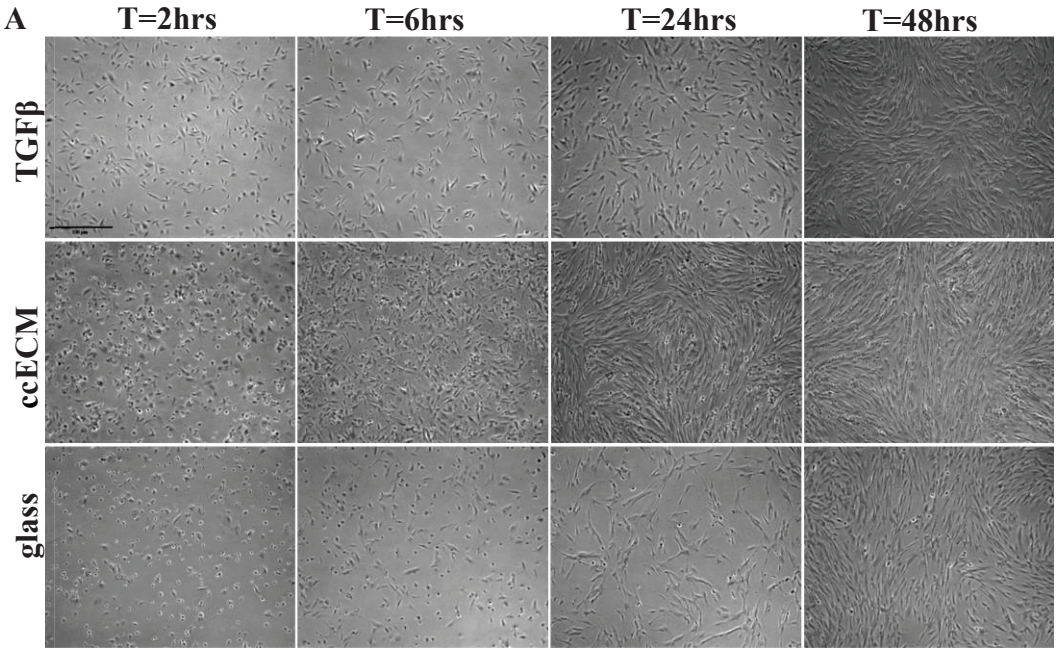

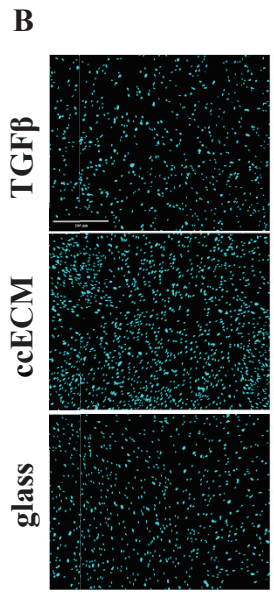

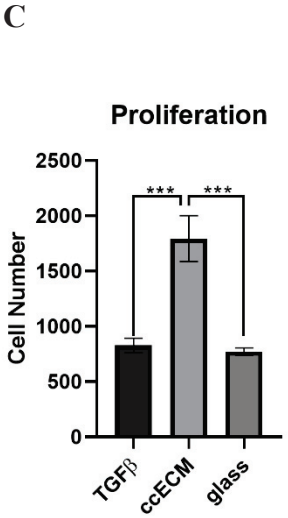

Figure 3.16.The fibroblasts' attachment on ccECM increased within 6 hours. A. Bright field images for fibroblast induced with 10ng/ml TGFβ(upper), cultured on decellularized ccECM(middle), and cultured on the glass surface(bottom) with different time points(T=hour(2hrs-6hrs-24hrs-48hrs) from left to right). B. DAPI staining for determination of cell proliferation in fibroblast induced with 10ng/ml TGFβ(upper), cultured on ccECM(middle), and cultured on the glass surface(bottom) for 48hours. C. Cell number of DAPI counted slides(n=8). Images were taken by fluorescence microscopy with 5X magnification. Scale bar: 100μm. Statistical analysis was performed using unpaired t-test (* p<0,05; ** p<0,01; *** p<0,005 ; **** p< 0,0001). The error bars represent the standard error

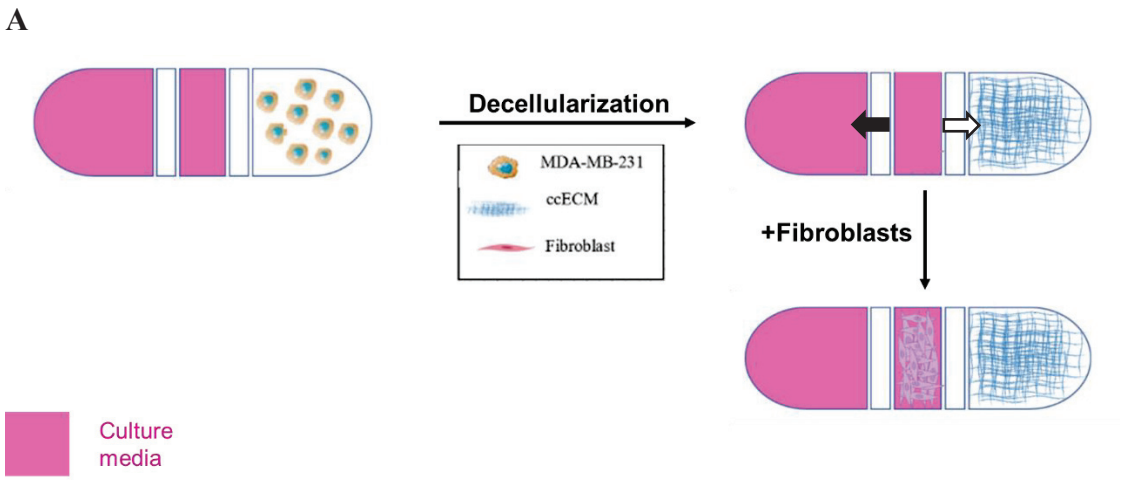

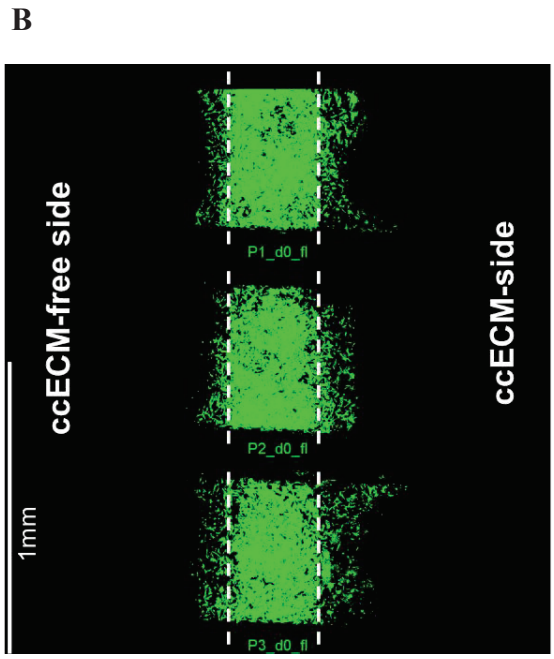

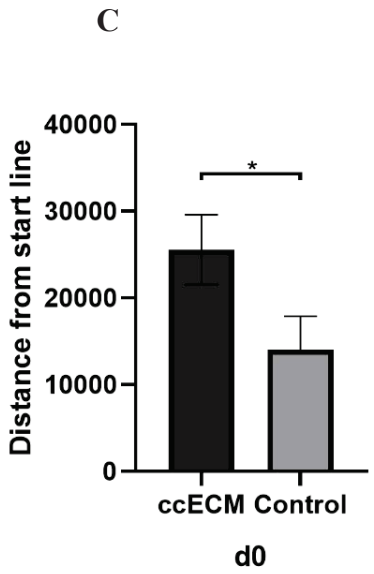

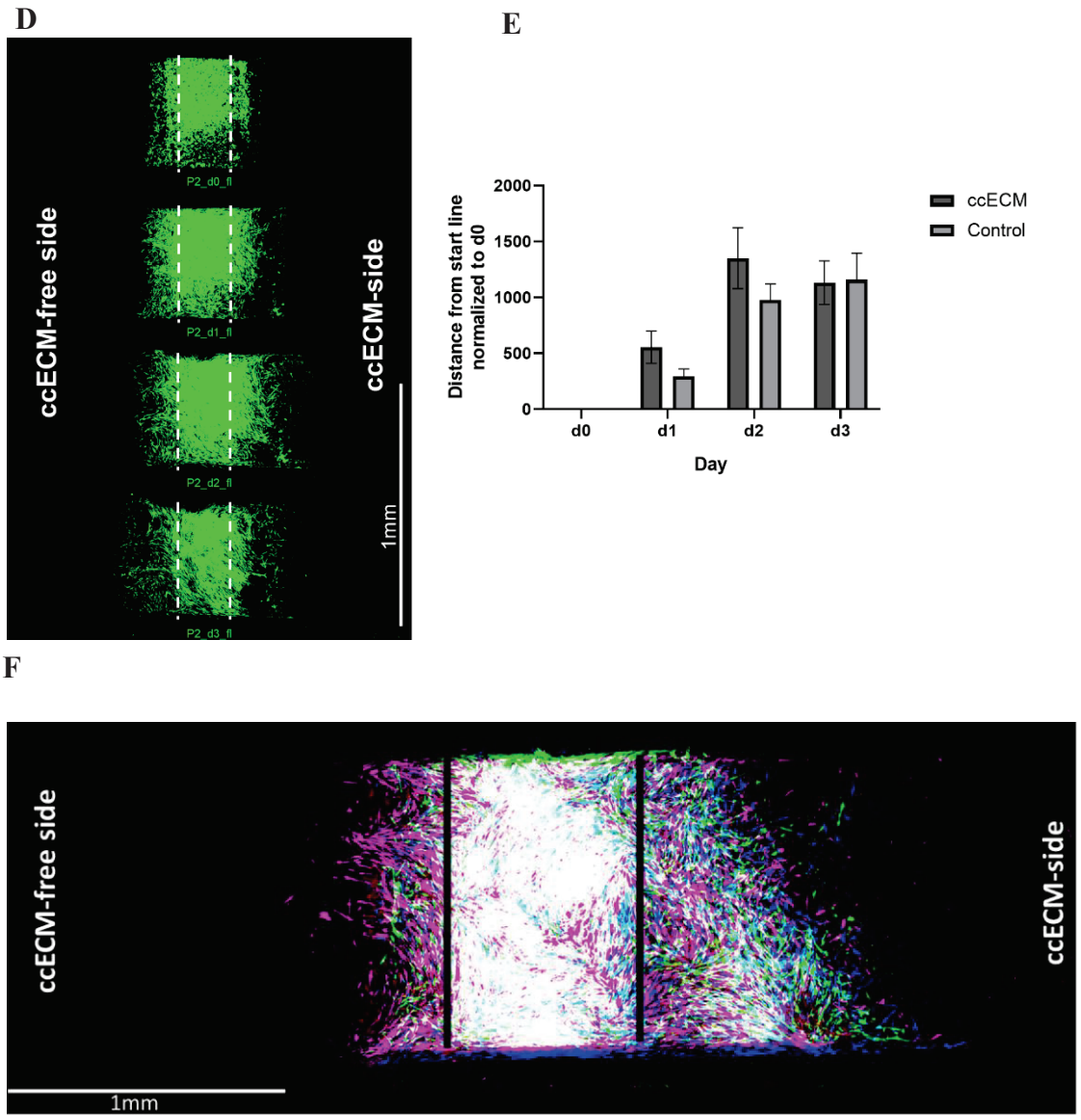

Figure 3.17. Observation of recruiting the fibroblast by the ccECM. A. Experimental design for migration using Biorender. B. Migration of the green-stained fibroblast towards either ccECM(right, white arrow) or control side(left, white arrow) at day0 from different positions (P represents different positions from the single LOC device: P1_d0_fl: Position1:day0:fluorescence). C. Sum of distance from the start line (straight white line) at day0. D. Day-dependent migration of fibroblast to either ccECM(right) or control side(left) on the same position (P2:Position2). E. Day-dependent sum of the distance from the start line (white straight line) normalized to d0. F. Migration of fibroblast towards ccECM and ccECM-free side. Each color represented a day (red:day0, green:day1, blue:day2, and magenta:day3). Images were taken by confocal microscopy with 10X magnification and created by ImageJ software using a montage section. Statistical analysis was performed using unpaired t-test (* $p<0,05$; ** $p<0,01$; *** $p<0,005$; **** $p< 0,0001$). The error bars represent the standard error.

CHAPTER 4.

DISCUSSION AND CONCLUSION

In this study, we investigated the fibroblast differentiation to CAFs at the cellular level utilizing ccECM decellularized from MDA-MB-231 by the freeze-thaw methods. Here, we found that decellularization using the extraction buffer was not as effective as the freeze-thaw. As far as our concern, this is due to ingredients present in the extraction buffer, such as ammonium hydroxide and triton X-100. Since they remove cell chemical and enzymatic processes, they may alter ECM components and microstructure. For instance, Verstegen M. and colleagues revealed that triton X-100 could reduce fibronectin and laminin on the decellularized ECM, disrupting dECM structure[124]. In our experiments, we also did not achieve a compact and well-organized ccECM structure when the extraction buffer was used for decellularization(Figure 3.4). Although the freeze-thaw cycle has disadvantages for purifying cell-free nuclei, additional processes like treating with DNAse compensate for this stiuation[101], as shown (Figure 3.6B, left).

We, first, quantitatively determined ECM depositions on ccECM using coomassie blue staining(Figure 3.3). After approving our decellularization method, we checked ECM components using immunostaining, including fibronectin and laminin. We found a statistically significant intensity compared to the glass surface(Figure 3.7). This significance also supported the power of the freeze-thaw method for the decellularization of ccECM.

Until here, we understood that the freeze-thaw method could deposit ECM components from MDA-MB-231 cells after five days of culturing. In order to determine for culture day to obtain ccECM from MDA-MB-231 cells, we tried 3-5-7 days. Our SEM results(Figure 3.4 and 3.5) showed that the best structure for ccECM was comprised at day 5, indicating that there might be a turnover of ECM production within a specific time. In that study, we claimed that MDA-MB-231 cells begin to produce ECM depositions and leave it to the surface on day 3. Then it reached a compact, well-organized structure on day 5. Furthermore, it started disintegrating after day 5 and completely disrupted on

day 7(data not shown). Hence, we used ccECM from 5 days of cultured MDA-MB-231 for our subsequent experiments.

The next step was the central part of the experiments. We investigated the differentiation of the fibroblast cultured on ccECM to CAFs by measuring CAF markers at the cellular and molecular levels. We used standard CAF markers in the literature, including vimentin, FAP, PDGFRβ, α-SMA, and FSP1/s100A4, CD29[65]. We also included fibronectin and laminin to see whether activated fibroblasts increase the expression of these ECM components[73]. At protein expression levels, all markers except for FSP1 increased significantly. The first marker that we checked was vimentin. Although there was fluctuating about being CAFs marker for vimentin, several papers indicated that vimentin expression increased when they co-cultured cancer cells with the fibroblast, which resulted from differentiation of fibroblast to CAF[125, 126].

Moreover, patients with vimentin-positive CAFs had shorter overall survival and poor prognosis[127]. In several papers, it was indicated that vimentin expression was confluency dependent. David Sarrio in 2008 and K Vuoriluoto in 2011 found that vimentin expression was increased as the confluency decrease[128, 129]. Therefore we suspected whether we obtained false-positive results from vimentin expression in our experiments(Figure 3.8B). To investigate this situation, we performed one experiment seeding different cell numbers of fibroblast for ccECM and control groups. We also found that significant increase for vimentin when they seeded at 5208 cells/cm^2 and 52080 cells/^{2} for low(Figure 4A) and high(Figure 4B) confluency. Then, we performed immunostaining upon vimentin, and our results showed that regardless of confluency, vimentin expression was higher in the fibroblasts seeding on ccECM compared to control groups(Figure 4C, n=1, * $p<0.05$). In addition to our test condition, TGFβ-induced fibroblasts were activated and positive for vimentin as exppected[130], suggesting contents of ccECM can create a similar effect as in TGFβ.

In the light of our results, we also showed that the FAP expression in fibroblasts on the ccECM and TGFβ induced cells was highly overexpressed compared to control groups. As indicated in the literature, FAP is one of the prominent markers for characterizing CAFs[114]. Overexpression of FAP was almost found in all tumor types, especially in their interstitium[131], a barrier between membranes and organs, suggesting the ECM components impact FAP markers. That is why the increased expression of FAP

in our fibroblasts on ccECM could result from factors including chemokine and cytokine present in ccECM.

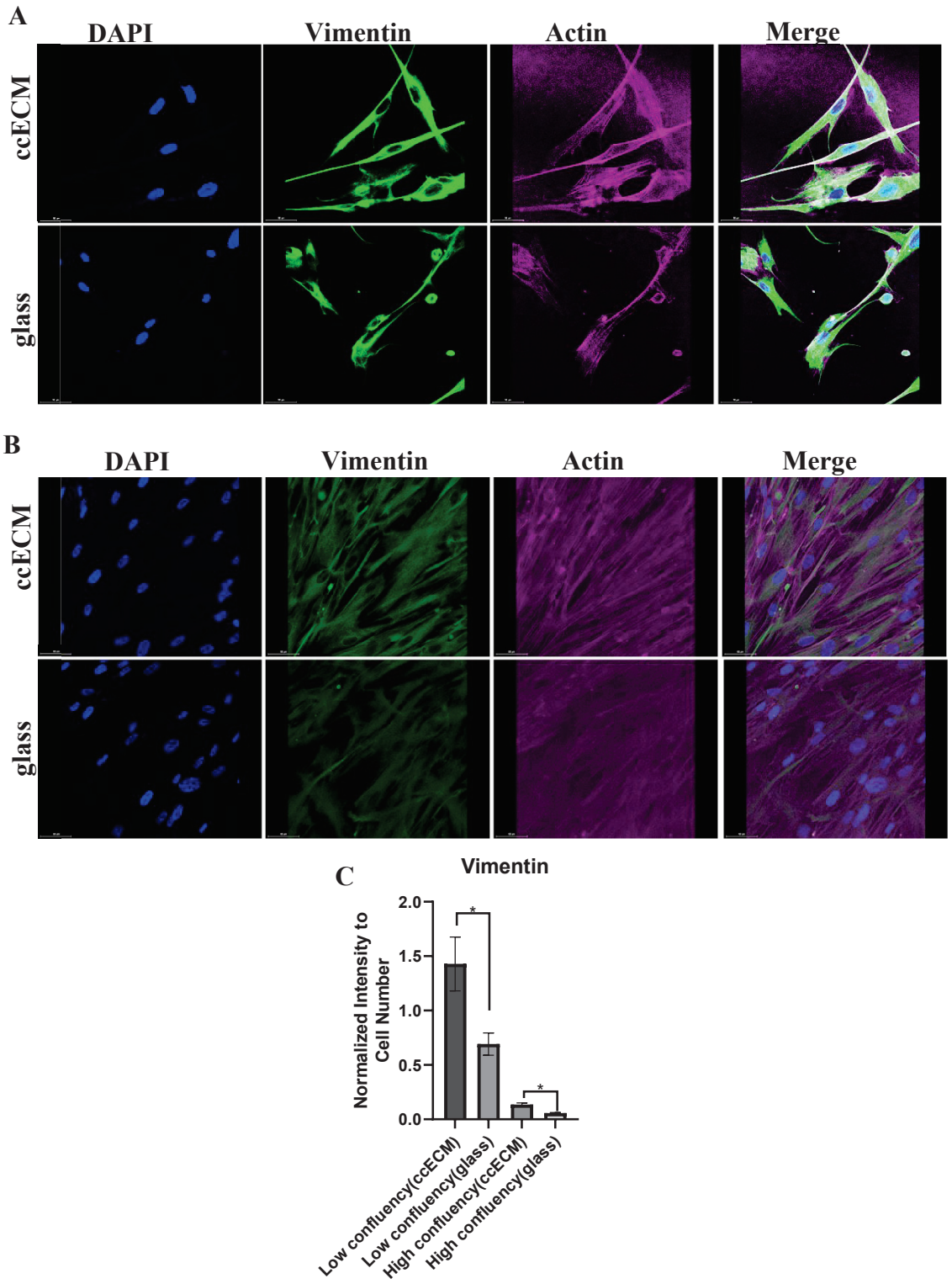

Figure 4. 1. Effect of the confluency on the vimentin expression on ccECM and glass surface. A. At low density, vimentin expression in the fibroblasts seeded

Figure 4.1-(cont) on ccECM and glass. B. At high density, vimentin expression in the fibroblasts.seeded on ccECM and glass. Images were taken by confocal microscopy with 40X magnification. Cell nuclei were stained with DAPI and represented with blue(1st line), vimentin intensity was represented with green(2nd line), and actin was stained with Alexa Fluor 647 conjugated phalloidin and represented with magenta(3rd line). Scale bar: 50μm. C. Green intensity for laminin normalized to cell number(n=1). Statistical analysis was performed using unpaired t-test (* p<0,05; ** p<0,01; *** p<0,005 ; **** p< 0,0001). The error bars represent the standard error

Another marker was PDGF, which has two main receptors, PDGFRα and PDGFRβ. This receptor family impacts various cellular events, including proliferation and chemotaxis of fibroblasts, affecting cytoskeleton arranging and cell migration. Since they have tyrosine kinase activity, they highly regulate these cellular events via activating the phosphoinositide 3-kinase (PI3K) and the mitogen-activated protein kinase (MAPK)[132]. Hence, it has been considered a CAFs marker in several studies[118]. Here, we also presented that PDGFRβ was more pronounced in our test conditions when the fibroblast was seeded on the ccECM(Figure 3.10B), indicating that PDGF may be found bound to the ccECM surface.

α-SMA, also known as ACTA2, is the most common marker to verify CAFs when the fibroblasts are induced with TGFβ[71, 72]. Here, we also found more a-SMA expression in TGFβ-induced groups but not in fibroblasts cultured on ccECM. Yet, several works informed a-SMA negative, FAP positive CAFs[65], as shown in our study(Figure 3.11B, 3.9B). These CAFs mostly attributed as immunosuppressive and mediate cancer cells hijacking from cellular immune system[133].

Another protein used for CAFs characterization belongs to the calcium-binding s100 protein family called FSP1/s100A4. In spite of the fact that FSP1 is one of the CAF markers, recent studies have indicated expression of FSP1 varies in different CAFs population[134, 135]. Based on our studies, we did not find significant changes in FSP1 expression at protein level not only between ccECM and control but also no changes in TGFβ induced cells compared to ccECM and control groups(Figure 3.12B).

In addition to CAFs markers, we also checked less pronounced markers in CAFS, which were laminin and fibronectin[73]. In our experimental setup, fibronectin did not change in ccECM fibroblasts compared to control groups but not TGFβ induced cells. It

was significantly decreased in the fibroblast on ccECM than TGFβ induced cells. Similarly, laminin expression in ccECM fibroblast was significantly lower compared to control and TGFβ induced groups. Hence, we came up with the idea that there could be negative feedback considering ccECM conditions since it already had these ECM components in its structure(Figure 3.7).

Another aspect of our study relied on relative mRNA expression of these CAFs markers, including CD29. According to our results, none of our markers showed significant change in the fibroblasts cultured on ccECM compared to control groups. When we compared ccECM and TGFβ induced cells, we found that while a-SMA(ns), FAP, and CD29 were decreased, FSP1 was increased at relative mRNA expression in ccECM groups(Table 4.1). Additionally, TGFb-induced cells had higher mRNA expression for a-SMA, FAP, and CD29, while FSP1 decreased (Table 4.1).

dECM not only comprises ECM components such as collagens, laminin, and fibronectin but also has several factors, including growth factors, chemokines, and cytkonies[101, 103, 136]. Moreover, these components may change when the cells become cancerous, and the ECM accumulates different factors compared to its healthy counterpart[137, 138]. Therefore, expecting the same results in the fibroblasts cultured on ccECM and TGFβ-induced cells could be a misapprehension concerning CAF markers. Since the factors present in ccECM may affect the translation of these proteins, the half-life of mRNA could be different from other groups, yielding increased protein expression but not mRNA[139](Table4.1).

Until here, we showed the freeze-thaw method provided proper decellularization for creating ccECM from MDA-MB-231 after culturing for 5 days. In addition to decellularization, we also indicated the way for the recellularization of the fibroblasts on the ccECM to investigate fibroblast differentiation into CAFs. Surprisingly, we came across a situation showing that the fibroblast seeded on ccECM had more proliferative than others(Figure3.16). It was shown in a study published in 2020 by Karina M. and colleagues when they cultured fibroblast and CAFs on the fibronectin-rich matrix[140]. Since our ccECM had significant fibronectin, it might affect the fibroblasts' proliferation when cultured on fibronectin-rich ccECM(Figure 3.3.2A, left).

Finally, we desired to investigate whether the ccECM had an impact on recruiting the fibroblasts using the LOC device, enabling the migration of cells from a start line (Figure3.17).

Table 4. 1 Summary of the expression of CAFs markers based on our results.

	Protein Level	mRNA Level
Vimentin	↑ ⇔ ↑	↔ ⇔ ↔
FAP	↑ ⇧ ↑	↔ ⇩ ↑
PDGFRβ	↑ ⇧ ↑	↔ ⇔ ↔
α-SMA/ACTA2	↔ ⇩ ↑	↔ ⇩ ns ↑
FSP1/s100A4	↔ ⇔ ↔	↔ ⇧ ↓
Fibronectin	↔ ⇩ ↔	Unchecked
Laminin	↓ ⇩ ↔	Unchecked
CD29/ITGB1	Unchecked	↔ ⇩ ↑

ccECM to control
ccECM to TGFβ
TGFβ to control

Interestingly, the fibroblasts migrated towards the ccECM side within 3 hours(day0) after seeding on that system(Figure 3.17B). However, their migration capacity to the ccECM side did not show significance as time passed. Instead, they also preferred to migrate to the control side, filled with their medium(Figure3.17C).

We found that the freeze-thaw method was more appropriate than the extraction buffer when one wants to create decellularized cell-free ECM. The ccECM decellularized by the freeze-thaw was more compact and well organized. It had high laminin and fibronectin, providing more proliferative for the fibroblasts.

Overall, the ccECM decellularized by the freeze-thaw was more compact and well organized than the one prepared by the extraction buffer. DNAse treatment remarkably eliminated cell-free nuclei, and ccECM contained fibronectin and laminin. ccECM was capable of differentiating fibroblasts to CAFs as determined by the expression of markers of CAFs. ccECM enhanced the proliferation and presence of actin fibers of CAFs, and it appears to orient the migration of fibroblasts. ccECM could be one of the intermediate

steps in fibroblast differentiation, but in the future, the factors present in ccECM should scrutinize to understand the mechanisms behind this transdifferentiation.

REFERENCES

1. Bray, F.; Laversanne, M.; Weiderpass, E.; Soerjomataram, I., The ever-increasing importance of cancer as a leading cause of premature death worldwide. *Cancer* **2021,** *127* (16), 3029-3030.

2. Sung, H.; Ferlay, J.; Siegel, R. L.; Laversanne, M.; Soerjomataram, I.; Jemal, A.; Bray, F., Global Cancer Statistics 2020: GLOBOCAN Estimates of Incidence and Mortality Worldwide for 36 Cancers in 185 Countries. *CA Cancer J Clin* **2021,** *71* (3), 209-249.

3. Stratton, M. R.; Campbell, P. J.; Futreal, P. A., The cancer genome. *Nature* **2009,** *458* (7239), 719-724.

4. Evan, G. I.; Vousden, K. H., Proliferation, cell cycle and apoptosis in cancer. *nature* **2001,** *411* (6835), 342-348.

5. Pavel, M.; Renna, M.; Park, S. J.; Menzies, F. M.; Ricketts, T.; Füllgrabe, J.; Ashkenazi, A.; Frake, R. A.; Lombarte, A. C.; Bento, C. F., Contact inhibition controls cell survival and proliferation via YAP/TAZ-autophagy axis. *Nature communications* **2018,** *9* (1), 1-18.

6. Hanahan, D., Hallmarks of Cancer: New Dimensions. *Cancer Discov* **2022,** *12* (1), 31-46.

7. Forouzanfar, M. H.; Foreman, K. J.; Delossantos, A. M.; Lozano, R.; Lopez, A. D.; Murray, C. J.; Naghavi, M., Breast and cervical cancer in 187 countries between 1980 and 2010: a systematic analysis. *The lancet* **2011,** *378* (9801), 1461-1484.

8. Feng, Y.; Spezia, M.; Huang, S.; Yuan, C.; Zeng, Z.; Zhang, L.; Ji, X.; Liu, W.; Huang, B.; Luo, W.; Liu, B.; Lei, Y.; Du, S.; Vuppalapati, A.; Luu, H. H.; Haydon, R. C.; He, T. C.; Ren, G., Breast cancer development and progression: Risk factors, cancer stem cells, signaling pathways, genomics, and molecular pathogenesis. *Genes Dis* **2018,** *5* (2), 77-106.

9. Harbeck, N.; Penault-Llorca, F.; Cortes, J.; Gnant, M.; Houssami, N.; Poortmans, P.; Ruddy, K.; Tsang, J.; Cardoso, F., Breast cancer. *Nat Rev Dis Primers* **2019,** *5* (1), 66.

10. Loibl, S.; Poortmans, P.; Morrow, M.; Denkert, C.; Curigliano, G., Breast cancer. *The Lancet* **2021,** *397* (10286), 1750-1769.

11. Kuchenbaecker, K. B.; Hopper, J. L.; Barnes, D. R.; Phillips, K.-A.; Mooij, T. M.; Roos-Blom, M.-J.; Jervis, S.; Van Leeuwen, F. E.; Milne, R. L.; Andrieu, N., Risks of breast, ovarian, and contralateral breast cancer for BRCA1 and BRCA2 mutation carriers. *Jama* **2017,** *317* (23), 2402-2416.

12. Taylor, A.; Brady, A. F.; Frayling, I. M.; Hanson, H.; Tischkowitz, M.; Turnbull, C.; Side, L., Consensus for genes to be included on cancer panel tests offered by UK genetics services: guidelines of the UK Cancer Genetics Group. *Journal of medical genetics* **2018,** *55* (6), 372-377.

13. Kamińska, M.; Ciszewski, T.; Łopacka-Szatan, K.; Miotła, P.; Starosławska, E., Breast cancer risk factors. *Menopause Review/Przegląd Menopauzalny* **2015,** *14* (3), 196-202.

14. Bombonati, A.; Sgroi, D. C., The molecular pathology of breast cancer progression. *The Journal of pathology* **2011,** *223* (2), 308-318.

15. Kakarala, M.; Wicha, M. S., Implications of the cancer stem-cell hypothesis for breast cancer prevention and therapy. *Journal of clinical oncology: official journal of the American Society of Clinical Oncology* **2008,** *26* (17), 2813.

16. Zucca-Matthes, G.; Urban, C.; Vallejo, A., Anatomy of the nipple and breast ducts. *Gland surgery* **2016,** *5* (1), 32.

17. Pinder, S. E.; Ellis, I. O., The diagnosis and management of pre-invasive breast disease: ductal carcinoma in situ (DCIS) and atypical ductal hyperplasia (ADH)–current definitions and classification. *Breast Cancer Research* **2003,** *5* (5), 1-4.

18. Wellings, S.; Jensen, H. M.; Marcum, R., An atlas of subgross pathology of the human breast with special reference to possible precancerous lesions. *Journal of the National Cancer Institute* **1975,** *55* (2), 231-273.

19. Sgroi, D. C., Preinvasive breast cancer. *Annu Rev Pathol* **2010,** *5*, 193-221.

20. Perou, C. M.; Sørlie, T.; Eisen, M. B.; Van De Rijn, M.; Jeffrey, S. S.; Rees, C. A.; Pollack, J. R.; Ross, D. T.; Johnsen, H.; Akslen, L. A., Molecular portraits of human breast tumours. *nature* **2000,** *406* (6797), 747-752.

21. Cheang, M. C.; Martin, M.; Nielsen, T. O.; Prat, A.; Voduc, D.; Rodriguez-Lescure, A.; Ruiz, A.; Chia, S.; Shepherd, L.; Ruiz-Borrego, M., Defining breast cancer intrinsic subtypes by quantitative receptor expression. *The oncologist* **2015,** *20* (5), 474-482.

22. Pommier, R. M.; Sanlaville, A.; Tonon, L.; Kielbassa, J.; Thomas, E.; Ferrari, A.; Sertier, A.-S.; Hollande, F.; Martinez, P.; Tissier, A., Comprehensive characterization of claudin-low breast tumors reflects the impact of the cell-of-origin on cancer evolution. *Nature communications* **2020,** *11* (1), 1-12.

23. Dai, X.; Cheng, H.; Bai, Z.; Li, J., Breast cancer cell line classification and its relevance with breast tumor subtyping. *Journal of Cancer* **2017,** *8* (16), 3131.

24. Valkenburg, K. C.; de Groot, A. E.; Pienta, K. J., Targeting the tumour stroma to improve cancer therapy. *Nature Reviews Clinical Oncology* **2018,** *15* (6), 366-381.

25. Denton, A. E.; Roberts, E. W.; Fearon, D. T., Stromal Cells in the Tumor Microenvironment. *Adv Exp Med Biol* **2018,** *1060*, 99-114.

26. Paget, S., The distribution of secondary growths in cancer of the breast. *The Lancet* **1889,** *133* (3421), 571-573.

27. Mammoto, T.; Ingber, D. E., Mechanical control of tissue and organ development. *Development* **2010,** *137* (9), 1407-1420.

28. Talmadge, J. E.; Donkor, M.; Scholar, E., Inflammatory cell infiltration of tumors: Jekyll or Hyde. *Cancer and Metastasis Reviews* **2007,** *26* (3), 373-400.

29. Bingle, L.; Brown, N.; Lewis, C. E., The role of tumour-associated macrophages in tumour progression: implications for new anticancer therapies. *The Journal of Pathology: A Journal of the Pathological Society of Great Britain and Ireland* **2002,** *196* (3), 254-265.

30. Murdoch, C.; Muthana, M.; Coffelt, S. B.; Lewis, C. E., The role of myeloid cells in the promotion of tumour angiogenesis. *Nature reviews cancer* **2008,** *8* (8), 618-631.

31. Gordon, S., Alternative activation of macrophages. *Nature reviews immunology* **2003,** *3* (1), 23-35.

32. Mantovani, A.; Sica, A.; Sozzani, S.; Allavena, P.; Vecchi, A.; Locati, M., The chemokine system in diverse forms of macrophage activation and polarization. *Trends in immunology* **2004,** *25* (12), 677-686.

33. Mosser, D. M.; Edwards, J. P., Exploring the full spectrum of macrophage activation. *Nature reviews immunology* **2008,** *8* (12), 958-969.

34. Folkman, J. In *Role of angiogenesis in tumor growth and metastasis*, Seminars in oncology, Elsevier: 2002; pp 15-18.

35. Gerhardt, H.; Semb, H., Pericytes: gatekeepers in tumour cell metastasis? *Journal of molecular medicine* **2008,** *86* (2), 135-144.

36. Vivier, E.; Tomasello, E.; Baratin, M.; Walzer, T.; Ugolini, S., Functions of natural killer cells. *Nature immunology* **2008,** *9* (5), 503-510.

37. Virchow, R., *Die Cellularpathologie in ihrer Begründung auf physiologische und pathologische Gewebelehre: zwanzig Vorlesungen, gehalten während der Monate Februar, März und April 1858 im pathologischen Institute zu Berlin*. Hirschwald: 1859; Vol. 1.

38. Duval, M., *Atlas d'embryologie*. G. Masson: 1889.

39. Tarin, D.; Croft, C., Ultrastructural features of wound healing in mouse skin. *Journal of anatomy* **1969,** *105* (Pt 1), 189-190.

40. Kalluri, R., The biology and function of fibroblasts in cancer. *Nat Rev Cancer* **2016,** *16* (9), 582-98.

41. Strutz, F.; Okada, H.; Lo, C. W.; Danoff, T.; Carone, R. L.; Tomaszewski, J. E.; Neilson, E. G., Identification and characterization of a fibroblast marker: FSP1. *The Journal of cell biology* **1995,** *130* (2), 393-405.

42. Hematti, P., Mesenchymal stromal cells and fibroblasts: a case of mistaken identity? *Cytotherapy* **2012,** *14* (5), 516-521.

43. Kalluri, R., The biology and function of fibroblasts in cancer. *Nature Reviews Cancer* **2016,** *16* (9), 582-598.

44. Kalluri, R.; Zeisberg, M., Fibroblasts in cancer. *Nat Rev Cancer* **2006,** *6* (5), 392-401.

45. Tomasek, J. J.; Gabbiani, G.; Hinz, B.; Chaponnier, C.; Brown, R. A., Myofibroblasts and mechano-regulation of connective tissue remodelling. *Nature reviews Molecular cell biology* **2002,** *3* (5), 349-363.

46. Parsonage, G.; Filer, A. D.; Haworth, O.; Nash, G. B.; Rainger, G. E.; Salmon, M.; Buckley, C. D., A stromal address code defined by fibroblasts. *Trends in immunology* **2005,** *26* (3), 150-156.

47. Rodemann, H. P.; Müller, G. A., Characterization of human renal fibroblasts in health and disease: II. In vitro growth, differentiation, and collagen synthesis of fibroblasts from kidneys with interstitial fibrosis. *American Journal of Kidney Diseases* **1991,** *17* (6), 684-686.

48. Chang, H. Y.; Chi, J.-T.; Dudoit, S.; Bondre, C.; van de Rijn, M.; Botstein, D.; Brown, P. O., Diversity, topographic differentiation, and positional memory in human fibroblasts. *Proceedings of the National Academy of Sciences* **2002,** *99* (20), 12877-12882.

49. Simian, M.; Hirai, Y.; Navre, M.; Werb, Z.; Lochter, A.; Bissell, M. J., The interplay of matrix metalloproteinases, morphogens and growth factors is necessary for branching of mammary epithelial cells. **2001**.

50. Wiseman, B. S.; Werb, Z., Stromal effects on mammary gland development and breast cancer. *Science* **2002,** *296* (5570), 1046-1049.

51. Elenbaas, B.; Weinberg, R. A., Heterotypic signaling between epithelial tumor cells and fibroblasts in carcinoma formation. *Experimental cell research* **2001,** *264* (1), 169-184.

52. Löhr, M.; Schmidt, C.; Ringel, J.; Kluth, M.; Müller, P.; Nizze, H.; Jesnowski, R., Transforming growth factor-β1 induces desmoplasia in an experimental model of human pancreatic carcinoma. *Cancer research* **2001,** *61* (2), 550-555.

53. Aoyagi, Y.; Oda, T.; Kinoshita, T.; Nakahashi, C.; Hasebe, T.; Ohkohchi, N.; Ochiai, A., Overexpression of TGF-β by infiltrated granulocytes correlates with the expression of collagen mRNA in pancreatic cancer. *British journal of cancer* **2004,** *91* (7), 1316-1326.

54. Mueller, M. M.; Fusenig, N. E., Friends or foes—bipolar effects of the tumour stroma in cancer. *Nature Reviews Cancer* **2004,** *4* (11), 839-849.

55. Lazard, D.; Sastre, X.; Frid, M. G.; Glukhova, M. A.; Thiery, J.-P.; Koteliansky, V., Expression of smooth muscle-specific proteins in myoepithelium and stromal myofibroblasts of normal and malignant human breast tissue. *Proceedings of the National Academy of Sciences* **1993,** *90* (3), 999-1003.

56. Rønnov-Jessen, L.; Petersen, O. W.; Koteliansky, V. E.; Bissell, M. J., The origin of the myofibroblasts in breast cancer. Recapitulation of tumor environment in culture unravels diversity and implicates converted fibroblasts and recruited smooth muscle cells. *The Journal of clinical investigation* **1995,** *95* (2), 859-873.

57. De Wever, O.; Demetter, P.; Mareel, M.; Bracke, M., Stromal myofibroblasts are drivers of invasive cancer growth. *International journal of cancer* **2008,** *123* (10), 2229-2238.

58. Tsujino, T.; Seshimo, I.; Yamamoto, H.; Ngan, C. Y.; Ezumi, K.; Takemasa, I.; Ikeda, M.; Sekimoto, M.; Matsuura, N.; Monden, M., Stromal myofibroblasts predict disease recurrence for colorectal cancer. *Clinical cancer research* **2007,** *13* (7), 2082-2090.

59. Laklai, H.; Miroshnikova, Y. A.; Pickup, M. W.; Collisson, E. A.; Kim, G. E.; Barrett, A. S.; Hill, R. C.; Lakins, J. N.; Schlaepfer, D. D.; Mouw, J. K., Genotype tunes pancreatic ductal adenocarcinoma tissue tension to induce matricellular fibrosis and tumor progression. *Nature medicine* **2016,** *22* (5), 497-505.

60. Calvo, F.; Ege, N.; Grande-Garcia, A.; Hooper, S.; Jenkins, R. P.; Chaudhry, S. I.; Harrington, K.; Williamson, P.; Moeendarbary, E.; Charras, G., Mechanotransduction and YAP-dependent matrix remodelling is required for the generation and maintenance of cancer-associated fibroblasts. *Nature cell biology* **2013,** *15* (6), 637-646.

61. Baeriswyl, V.; Christofori, G. In *The angiogenic switch in carcinogenesis*, Seminars in cancer biology, Elsevier: 2009; pp 329-337.

62. Flavell, R. A.; Sanjabi, S.; Wrzesinski, S. H.; Licona-Limón, P., The polarization of immune cells in the tumour environment by TGFβ. *Nature reviews immunology* **2010,** *10* (8), 554-567.

63. Kim, J. H.; Sun-Hee, O.; Kim, E.-J.; Park, S. J.; Hong, S. P.; Cheon, J. H.; Kim, T. I.; Kim, W. H., The role of myofibroblasts in upregulation of S100A8 and S100A9 and the differentiation of myeloid cells in the colorectal cancer

microenvironment. *Biochemical and biophysical research communications* **2012,** *423* (1), 60-66.

64. Yang, X.; Lin, Y.; Shi, Y.; Li, B.; Liu, W.; Yin, W.; Dang, Y.; Chu, Y.; Fan, J.; He, R., FAP promotes immunosuppression by cancer-associated fibroblasts in the tumor microenvironment via STAT3–CCL2 signaling. *Cancer research* **2016,** *76* (14), 4124-4135.

65. Mhaidly, R.; Mechta-Grigoriou, F., Role of cancer-associated fibroblast subpopulations in immune infiltration, as a new means of treatment in cancer. *Immunological reviews* **2021,** *302* (1), 259-272.

66. Celia-Terrassa, T.; Kang, Y., Distinctive properties of metastasis-initiating cells. *Genes Dev* **2016,** *30* (8), 892-908.

67. Cirri, P.; Chiarugi, P., Cancer associated fibroblasts: the dark side of the coin. *American journal of cancer research* **2011,** *1* (4), 482.

68. Rønnov-Jessen, L.; Petersen, O., Induction of alpha-smooth muscle actin by transforming growth factor-beta 1 in quiescent human breast gland fibroblasts. Implications for myofibroblast generation in breast neoplasia. *Laboratory investigation; a journal of technical methods and pathology* **1993,** *68* (6), 696-707.

69. Desmoulière, A.; Geinoz, A.; Gabbiani, F.; Gabbiani, G., Transforming growth factor-beta 1 induces alpha-smooth muscle actin expression in granulation tissue myofibroblasts and in quiescent and growing cultured fibroblasts. *The Journal of cell biology* **1993,** *122* (1), 103-111.

70. Kojima, Y.; Acar, A.; Eaton, E. N.; Mellody, K. T.; Scheel, C.; Ben-Porath, I.; Onder, T. T.; Wang, Z. C.; Richardson, A. L.; Weinberg, R. A., Autocrine TGF-β and stromal cell-derived factor-1 (SDF-1) signaling drives the evolution of tumor-promoting mammary stromal myofibroblasts. *Proceedings of the National Academy of Sciences* **2010,** *107* (46), 20009-20014.

71. Evans, R. A.; Tian, Y. C.; Steadman, R.; Phillips, A. O., TGF-β1-mediated fibroblast–myofibroblast terminal differentiation—the role of smad proteins. *Experimental cell research* **2003,** *282* (2), 90-100.

72. Thannickal, V. J.; Lee, D. Y.; White, E. S.; Cui, Z.; Larios, J. M.; Chacon, R.; Horowitz, J. C.; Day, R. M.; Thomas, P. E., Myofibroblast differentiation by transforming growth factor-beta1 is dependent on cell adhesion and integrin signaling via focal adhesion kinase. *J Biol Chem* **2003,** *278* (14), 12384-9.

73. Casey, T. M.; Eneman, J.; Crocker, A.; White, J.; Tessitore, J.; Stanley, M.; Harlow, S.; Bunn, J. Y.; Weaver, D.; Muss, H.; Plaut, K., Cancer associated fibroblasts stimulated by transforming growth factor beta1 (TGF-beta 1) increase invasion rate of tumor cells: a population study. *Breast Cancer Res Treat* **2008,** *110* (1), 39-49.

74. Guido, C.; Whitaker-Menezes, D.; Capparelli, C.; Balliet, R.; Lin, Z.; Pestell, R. G.; Howell, A.; Aquila, S.; Ando, S.; Martinez-Outschoorn, U.; Sotgia, F.; Lisanti, M. P., Metabolic reprogramming of cancer-associated fibroblasts by TGF-beta drives tumor growth: connecting TGF-beta signaling with "Warburg-like" cancer metabolism and L-lactate production. *Cell Cycle* **2012,** *11* (16), 3019-35.

75. Li, Q.; Zhang, D.; Wang, Y.; Sun, P.; Hou, X.; Larner, J.; Xiong, W.; Mi, J., MiR-21/Smad 7 signaling determines TGF-beta1-induced CAF formation. *Sci Rep* **2013,** *3*, 2038.

76. Yu, Y.; Xiao, C. H.; Tan, L. D.; Wang, Q. S.; Li, X. Q.; Feng, Y. M., Cancer-associated fibroblasts induce epithelial-mesenchymal transition of breast cancer cells through paracrine TGF-beta signalling. *Br J Cancer* **2014,** *110* (3), 724-32.

77. Shinde, A. V.; Humeres, C.; Frangogiannis, N. G., The role of alpha-smooth muscle actin in fibroblast-mediated matrix contraction and remodeling. *Biochim Biophys Acta Mol Basis Dis* **2017,** *1863* (1), 298-309.

78. Bordignon, P.; Bottoni, G.; Xu, X.; Popescu, A. S.; Truan, Z.; Guenova, E.; Kofler, L.; Jafari, P.; Ostano, P.; Rocken, M.; Neel, V.; Dotto, G. P., Dualism of FGF and TGF-beta Signaling in Heterogeneous Cancer-Associated Fibroblast Activation with ETV1 as a Critical Determinant. *Cell Rep* **2019,** *28* (9), 2358-2372 e6.

79. Mazumdar, A.; Urdinez, J.; Boro, A.; Migliavacca, J.; Arlt, M. J. E.; Muff, R.; Fuchs, B.; Snedeker, J. G.; Gvozdenovic, A., Osteosarcoma-Derived Extracellular Vesicles Induce Lung Fibroblast Reprogramming. *Int J Mol Sci* **2020,** *21* (15).

80. Yoon, H.; Tang, C. M.; Banerjee, S.; Delgado, A. L.; Yebra, M.; Davis, J.; Sicklick, J. K., TGF-beta1-mediated transition of resident fibroblasts to cancer-associated fibroblasts promotes cancer metastasis in gastrointestinal stromal tumor. *Oncogenesis* **2021,** *10* (2), 13.

81. William Petersen, O.; Lind Nielsen, H.; Gudjonsson, T.; Villadsen, R.; Rønnov-Jessen, L.; Bissell, M. J., The plasticity of human breast carcinoma cells is more than epithelial to mesenchymal conversion. *Breast Cancer Research* **2001,** *3* (4), 1-5.

82. Iwano, M.; Plieth, D.; Danoff, T. M.; Xue, C.; Okada, H.; Neilson, E. G., Evidence that fibroblasts derive from epithelium during tissue fibrosis. *The Journal of clinical investigation* **2002,** *110* (3), 341-350.

83. Lawson, W.; Zoia, O.; Polosukhin, V.; Blackwell, T. In *Evidence of epithelial mesenchymal transition in primary type II alveolar epithelial cells and mesothelial cells*, Proc Am Thorac Soc, 2005; p A853.

84. Willis, B. C.; duBois, R. M.; Borok, Z., Epithelial origin of myofibroblasts during fibrosis in the lung. *Proceedings of the American Thoracic Society* **2006,** *3* (4), 377-382.

85. Grünert, S.; Jechlinger, M.; Beug, H., Diverse cellular and molecular mechanisms contribute to epithelial plasticity and metastasis. *Nature reviews Molecular cell biology* **2003,** *4* (8), 657-665.

86. Watanabe-Takano, H.; Takano, K.; Hatano, M.; Tokuhisa, T.; Endo, T., DA-Raf-mediated suppression of the Ras—ERK pathway is essential for TGF-β1-induced epithelial—mesenchymal transition in alveolar epithelial Type 2 cells. *PLoS One* **2015,** *10* (5), e0127888.

87. Zeisberg, E. M.; Potenta, S.; Xie, L.; Zeisberg, M.; Kalluri, R., Discovery of endothelial to mesenchymal transition as a source for carcinoma-associated fibroblasts. *Cancer research* **2007,** *67* (21), 10123-10128.

88. Zeisberg, E. M.; Tarnavski, O.; Zeisberg, M.; Dorfman, A. L.; McMullen, J. R.; Gustafsson, E.; Chandraker, A.; Yuan, X.; Pu, W. T.; Roberts, A. B., Endothelial-to-mesenchymal transition contributes to cardiac fibrosis. *Nature medicine* **2007,** *13* (8), 952-961.

89. Potenta, S.; Zeisberg, E.; Kalluri, R., The role of endothelial-to-mesenchymal transition in cancer progression. *British journal of cancer* **2008,** *99* (9), 1375-1379.

90. Jotzu, C.; Alt, E.; Welte, G.; Li, J.; Hennessy, B. T.; Devarajan, E.; Krishnappa, S.; Pinilla, S.; Droll, L.; Song, Y.-H., Adipose tissue derived stem cells differentiate into carcinoma-associated fibroblast-like cells under the influence of tumor derived factors. *Cellular oncology* **2011,** *34* (1), 55-67.

91. Chen, X.; Song, E., Turning foes to friends: targeting cancer-associated fibroblasts. *Nat Rev Drug Discov* **2019,** *18* (2), 99-115.

92. Kieffer, Y.; Hocine, H. R.; Gentric, G.; Pelon, F.; Bernard, C.; Bourachot, B.; Lameiras, S.; Albergante, L.; Bonneau, C.; Guyard, A., Single-cell analysis reveals fibroblast clusters linked to immunotherapy resistance in cancer. *Cancer Discovery* **2020,** *10* (9), 1330-1351.

93. Bartoschek, M.; Oskolkov, N.; Bocci, M.; Lövrot, J.; Larsson, C.; Sommarin, M.; Madsen, C. D.; Lindgren, D.; Pekar, G.; Karlsson, G., Spatially and functionally distinct subclasses of breast cancer-associated fibroblasts revealed by single cell RNA sequencing. *Nature communications* **2018,** *9* (1), 1-13.

94. Costa, A.; Kieffer, Y.; Scholer-Dahirel, A.; Pelon, F.; Bourachot, B.; Cardon, M.; Sirven, P.; Magagna, I.; Fuhrmann, L.; Bernard, C., Fibroblast heterogeneity and immunosuppressive environment in human breast cancer. *Cancer cell* **2018,** *33* (3), 463-479. e10.

95. Bonneau, C.; Eliès, A.; Kieffer, Y.; Bourachot, B.; Ladoire, S.; Pelon, F.; Hequet, D.; Guinebretière, J.-M.; Blanchet, C.; Vincent-Salomon, A., A subset of activated fibroblasts is associated with distant relapse in early luminal breast cancer. *Breast Cancer Research* **2020,** *22* (1), 1-22.

96. Pelon, F.; Bourachot, B.; Kieffer, Y.; Magagna, I.; Mermet-Meillon, F.; Bonnet, I.; Costa, A.; Givel, A.-M.; Attieh, Y.; Barbazan, J., Cancer-associated fibroblast heterogeneity in axillary lymph nodes drives metastases in breast cancer through complementary mechanisms. *Nature communications* **2020,** *11* (1), 1-20.

97. Biffi, G.; Oni, T. E.; Spielman, B.; Hao, Y.; Elyada, E.; Park, Y.; Preall, J.; Tuveson, D. A., IL1-induced JAK/STAT signaling is antagonized by TGFβ to shape CAF heterogeneity in pancreatic ductal adenocarcinoma. *Cancer discovery* **2019,** *9* (2), 282-301.

98. Öhlund, D.; Handly-Santana, A.; Biffi, G.; Elyada, E.; Almeida, A. S.; Ponz-Sarvise, M.; Corbo, V.; Oni, T. E.; Hearn, S. A.; Lee, E. J., Distinct populations of inflammatory fibroblasts and myofibroblasts in pancreatic cancer. *Journal of Experimental Medicine* **2017,** *214* (3), 579-596.

99. Lambrechts, D.; Wauters, E.; Boeckx, B.; Aibar, S.; Nittner, D.; Burton, O.; Bassez, A.; Decaluwé, H.; Pircher, A.; Van den Eynde, K., Phenotype molding of stromal cells in the lung tumor microenvironment. *Nature medicine* **2018,** *24* (8), 1277-1289.

100. Hinderer, S.; Layland, S. L.; Schenke-Layland, K., ECM and ECM-like materials—Biomaterials for applications in regenerative medicine and cancer therapy. *Advanced drug delivery reviews* **2016,** *97*, 260-269.

101. Zhang, X.; Chen, X.; Hong, H.; Hu, R.; Liu, J.; Liu, C., Decellularized extracellular matrix scaffolds: Recent trends and emerging strategies in tissue engineering. *Bioact Mater* **2022,** *10*, 15-31.

102. Goh, S.-K.; Olsen, P.; Banerjee, I., Correction: Extracellular Matrix Aggregates from Differentiating Embryoid Bodies as a Scaffold to Support ESC Proliferation and Differentiation. *Plos one* **2013,** *8* (10).

103. Assuncao, M.; Dehghan-Baniani, D.; Yiu, C. H. K.; Spater, T.; Beyer, S.; Blocki, A., Cell-Derived Extracellular Matrix for Tissue Engineering and Regenerative Medicine. *Front Bioeng Biotechnol* **2020,** *8*, 602009.

104. Cukierman, E., Preparation of extracellular matrices produced by cultured fibroblasts. *Current protocols in cell biology* **2002,** *16* (1), 10.9. 1-10.9. 15.

105. Xing, Q.; Yates, K.; Tahtinen, M.; Shearier, E.; Qian, Z.; Zhao, F., Decellularization of fibroblast cell sheets for natural extracellular matrix scaffold preparation. *Tissue Engineering Part C: Methods* **2015,** *21* (1), 77-87.

106. Franco-Barraza, J.; Beacham, D. A.; Amatangelo, M. D.; Cukierman, E., Preparation of extracellular matrices produced by cultured and primary fibroblasts. *Current protocols in cell biology* **2016,** *71* (1), 10.9. 1-10.9. 34.

107. Hielscher, A. C.; Qiu, C.; Gerecht, S., Breast cancer cell-derived matrix supports vascular morphogenesis. *American Journal of Physiology-Cell Physiology* **2012,** *302* (8), C1243-C1256.

108. Machado Brandão-Costa, R.; Helal-Neto, E.; Maia Vieira, A.; Barcellos-de-Souza, P.; Morgado-Diaz, J.; Barja-Fidalgo, C., Extracellular matrix derived from high metastatic human breast cancer triggers epithelial-mesenchymal transition in epithelial breast cancer cells through αvβ3 integrin. *International journal of molecular sciences* **2020,** *21* (8), 2995.

109. Xing, Q.; Yates, K.; Tahtinen, M.; Shearier, E.; Qian, Z.; Zhao, F., Decellularization of fibroblast cell sheets for natural extracellular matrix scaffold preparation. *Tissue Eng Part C Methods* **2015,** *21* (1), 77-87.

110. Ferreira, L. P.; Gaspar, V. M.; Mano, J. F., Decellularized Extracellular Matrix for Bioengineering Physiomimetic 3D in Vitro Tumor Models. *Trends Biotechnol* **2020,** *38* (12), 1397-1414.

111. Gilpin, A.; Yang, Y., Decellularization Strategies for Regenerative Medicine: From Processing Techniques to Applications. *Biomed Res Int* **2017,** *2017*, 9831534.

112. Hoye, A. M.; Erler, J. T., Structural ECM components in the premetastatic and metastatic niche. *Am J Physiol Cell Physiol* **2016,** *310* (11), C955-67.

113. Nissen, N. I.; Karsdal, M.; Willumsen, N., Collagens and Cancer associated fibroblasts in the reactive stroma and its relation to Cancer biology. *J Exp Clin Cancer Res* **2019,** *38* (1), 115.

114. Han, C.; Liu, T.; Yin, R., Biomarkers for cancer-associated fibroblasts. *Biomark Res* **2020,** *8* (1), 64.

115. Sahai, E.; Astsaturov, I.; Cukierman, E.; DeNardo, D. G.; Egeblad, M.; Evans, R. M.; Fearon, D.; Greten, F. R.; Hingorani, S. R.; Hunter, T., A framework for advancing our understanding of cancer-associated fibroblasts. *Nature Reviews Cancer* **2020,** *20* (3), 174-186.

116. Ostrowska-Podhorodecka, Z.; Ding, I.; Norouzi, M.; McCulloch, C. A., Impact of Vimentin on Regulation of Cell Signaling and Matrix Remodeling. *Frontiers in Cell and Developmental Biology* **2022,** *10*, 869069-869069.

117. Kelly, T.; Huang, Y.; Simms, A. E.; Mazur, A., Fibroblast activation protein-α: a key modulator of the microenvironment in multiple pathologies. *International review of cell and molecular biology* **2012,** *297*, 83-116.

118. Donovan, J.; Shiwen, X.; Norman, J.; Abraham, D., Platelet-derived growth factor alpha and beta receptors have overlapping functional activities towards fibroblasts. *Fibrogenesis & tissue repair* **2013,** *6* (1), 1-9.

119. Wang, J.; Zohar, R.; McCulloch, C. A., Multiple roles of α-smooth muscle actin in mechanotransduction. *Experimental cell research* **2006,** *312* (3), 205-214.

120. Österreicher, C. H.; Penz-Österreicher, M.; Grivennikov, S. I.; Guma, M.; Koltsova, E. K.; Datz, C.; Sasik, R.; Hardiman, G.; Karin, M.; Brenner, D. A., Fibroblast-specific protein 1 identifies an inflammatory subpopulation of macrophages in the liver. *Proceedings of the National Academy of Sciences* **2011,** *108* (1), 308-313.

121. Boye, K.; Maelandsmo, G. M., S100A4 and metastasis: a small actor playing many roles. *Am J Pathol* **2010,** *176* (2), 528-35.

122. Parisi, L.; Toffoli, A.; Ghezzi, B.; Mozzoni, B.; Lumetti, S.; Macaluso, G. M., A glance on the role of fibronectin in controlling cell response at biomaterial interface. *Jpn Dent Sci Rev* **2020,** *56* (1), 50-55.

123. Aumailley, M., The laminin family. *Cell Adh Migr* **2013,** *7* (1), 48-55.

124. Verstegen, M. M.; Willemse, J.; Van Den Hoek, S.; Kremers, G.-J.; Luider, T. M.; van Huizen, N. A.; Willemssen, F. E.; Metselaar, H. J.; IJzermans, J. N.; van der Laan, L. J., Decellularization of whole human liver grafts using controlled perfusion for transplantable organ bioscaffolds. *Stem cells and development* **2017,** *26* (18), 1304-1315.

125. Ba, P.; Zhang, X.; Yu, M.; Li, L.; Duan, X.; Wang, M.; Lv, S.; Fu, G.; Yang, P.; Yang, C.; Sun, Q., Cancer associated fibroblasts are distinguishable from peri-tumor fibroblasts by biological characteristics in TSCC. *Oncol Lett* **2019,** *18* (3), 2484-2490.

126. Yu, T.; Guo, Z.; Fan, H.; Song, J.; Liu, Y.; Gao, Z.; Wang, Q., Cancer-associated fibroblasts promote non-small cell lung cancer cell invasion by upregulation of glucose-regulated protein 78 (GRP78) expression in an integrated bionic microfluidic device. *Oncotarget* **2016,** *7* (18), 25593.

127. Nomura, S., Identification, friend or foe: vimentin and α-smooth muscle actin in cancer-associated fibroblasts. *Annals of Surgical Oncology* **2019,** *26* (13), 4191-4192.

128. Sarrio, D.; Rodriguez-Pinilla, S. M.; Hardisson, D.; Cano, A.; Moreno-Bueno, G.; Palacios, J., Epithelial-mesenchymal transition in breast cancer relates to the basal-like phenotype. *Cancer Res* **2008,** *68* (4), 989-97.

129. Vuoriluoto, K.; Haugen, H.; Kiviluoto, S.; Mpindi, J. P.; Nevo, J.; Gjerdrum, C.; Tiron, C.; Lorens, J. B.; Ivaska, J., Vimentin regulates EMT induction by Slug and oncogenic H-Ras and migration by governing Axl expression in breast cancer. *Oncogene* **2011,** *30* (12), 1436-48.

130. Shiga, K.; Hara, M.; Nagasaki, T.; Sato, T.; Takahashi, H.; Takeyama, H., Cancer-Associated Fibroblasts: Their Characteristics and Their Roles in Tumor Growth. *Cancers (Basel)* **2015,** *7* (4), 2443-58.

131. Xin, L.; Gao, J.; Zheng, Z.; Chen, Y.; Lv, S.; Zhao, Z.; Yu, C.; Yang, X.; Zhang, R., Fibroblast Activation Protein-alpha as a Target in the Bench-to-Bedside Diagnosis and Treatment of Tumors: A Narrative Review. *Front Oncol* **2021,** *11*, 648187.

132. Aoto, K.; Ito, K.; Aoki, S., Complex formation between platelet-derived growth factor receptor β and transforming growth factor β receptor regulates the differentiation of mesenchymal stem cells into cancer-associated fibroblasts. *Oncotarget* **2018,** *9* (75), 34090.

133. Yang, X.; Lin, Y.; Shi, Y.; Li, B.; Liu, W.; Yin, W.; Dang, Y.; Chu, Y.; Fan, J.; He, R., FAP Promotes Immunosuppression by Cancer-Associated Fibroblasts in the Tumor Microenvironment via STAT3–CCL2 SignalingFAP via STAT3–CCL2 Promote Tumor Immunosuppression. *Cancer research* **2016,** *76* (14), 4124-4135.

134. Nurmik, M.; Ullmann, P.; Rodriguez, F.; Haan, S.; Letellier, E., In search of definitions: Cancer-associated fibroblasts and their markers. *Int J Cancer* **2020,** *146* (4), 895-905.

135. Friedman, G.; Levi-Galibov, O.; David, E.; Bornstein, C.; Giladi, A.; Dadiani, M.; Mayo, A.; Halperin, C.; Pevsner-Fischer, M.; Lavon, H.; Mayer, S.; Nevo, R.; Stein, Y.; Balint-Lahat, N.; Barshack, I.; Ali, H. R.; Caldas, C.; Nili-Gal-Yam, E.; Alon, U.; Amit, I.; Scherz-Shouval, R., Cancer-associated fibroblast compositions change with breast cancer progression linking the ratio of S100A4(+) and PDPN(+) CAFs to clinical outcome. *Nat Cancer* **2020,** *1* (7), 692-708.

136. Winkler, J.; Abisoye-Ogunniyan, A.; Metcalf, K. J.; Werb, Z., Concepts of extracellular matrix remodelling in tumour progression and metastasis. *Nat Commun* **2020,** *11* (1), 5120.

137. Xiong, G.-F.; Xu, R., Function of cancer cell-derived extracellular matrix in tumor progression. *Journal of Cancer Metastasis and Treatment* **2016,** *2* (9).

138. Poltavets, V.; Kochetkova, M.; Pitson, S. M.; Samuel, M. S., The Role of the Extracellular Matrix and Its Molecular and Cellular Regulators in Cancer Cell Plasticity. *Front Oncol* **2018,** *8*, 431.

139. Vogel, C.; Marcotte, E. M., Insights into the regulation of protein abundance from proteomic and transcriptomic analyses. *Nature reviews genetics* **2012,** *13* (4), 227-232.

140. Lugo-Cintrón, K. M.; Gong, M. M.; Ayuso, J. M.; Tomko, L. A.; Beebe, D. J.; Virumbrales-Muñoz, M.; Ponik, S. M., Breast fibroblasts and ECM components modulate breast cancer cell migration through the secretion of MMPs in a 3D microfluidic co-culture model. *Cancers* **2020,** *12* (5), 1173.